eng

MDPI

Article

Co-Pyrolysis of Urban Biosolids with Rice Husk and Pruning Waste: Effects on Biochar Quality, Stability and Agricultural Applicability

Luz María Landa-Zavaleta [1], Claudia Adriana Ramírez-Valdespino [2], Omar S. Castillo-Baltazar [3], David Aarón Rodríguez-Alejandro [4], César Leyva-Porras [5], María de la Luz Xochilt Negrete-Rodríguez [1], Honorio Patiño-Galván [1], Dioselina Álvarez-Bernal [6], Marcos Alfonso Lastiri-Hernández [7] and Eloy Conde-Barajas [1,*]

[1] Departamento de Posgrado de Ingeniería Bioquímica, Tecnológico Nacional de México/IT de Celaya, Ave. Tecnológico y A. García Cubas No. 600, Celaya 38010, Guanajuato, Mexico; luzmaria.landa@gmail.com (L.M.L.-Z.); xochilt.negrete@itcelaya.edu.mx (M.d.l.L.X.N.-R.); honorpg19@gmail.com (H.P.-G.)
[2] Centro de Investigaciones Biológicas del Noroeste (CIBNOR), Av. Instituto Politécnico Nacional 195, Playa Palo de Santa Rita Sur, La Paz 23096, Baja California Sur, Mexico; cvaldespino@cibnor.mx
[3] Departamento de Ingeniería Agroindustrial, Universidad de Guanajuato, Campus Celaya-Salvatierra, Ing. Francisco Javier Sierra 201, Ejido Santa María del Refugio, Celaya 38140, Guanajuato, Mexico; omar.castillo@ugto.mx
[4] Departamento de Ingeniería Mecánica, Universidad de Guanajuato, Campus Irapuato-Salamanca, Carretera Salamanca-Valle de Santiago km. 3.5 + 18 Comunidad de Palo Blanco, Salamanca 36885, Guanajuato, Mexico; da.rodriguez@ugto.mx
[5] Laboratorio Nacional de Nanotecnología, Centro de Investigación en Materiales Avanzados S.C. (CIMAV), Miguel de Cervantes No. 120, Complejo Industrial, Chihuahua 31136, Chihuahua, Mexico; cesar.leyva@cimav.edu.mx
[6] Centro Interdisciplinario de la Investigación para el Desarrollo Integral de la Región IPN, Justo Sierra No. 28, Jiquilpan 59510, Michoacán, Mexico; dalvarez@ipn.mx
[7] Tecnológico Nacional de México/ITS Los Reyes, Carretera Los Reyes-Jacona Km. 3, Los Reyes 60300, Michoacán, Mexico; marcos.lh@losreyes.tecnm.mx
* Correspondence: eloy.conde@itcelaya.edu.mx

Abstract

This study assessed the production and characterisation of biochars derived from the pyrolysis and co-pyrolysis of urban biosolids (BSs) combined with two lignocellulosic biomasses: rice husk (RH) and pruning waste (PW). The treatments were conducted at 300, 400, and 500 °C to evaluate the influence of temperature and mass ratio on the physicochemical, structural, and biological properties of the material. Co-pyrolysis significantly improved the material's properties, enhancing carbon content, surface area, porosity, and pH, while reducing ash and heavy metal concentrations. RH promoted greater porosity and alkalinity, whereas PW increased carbon content and improved maize germination. Biochars produced at 400–500 °C met the stability criterion (H/C < 0.7) set by the International Biochar Initiative (IBI) and the European Biochar Certificate (EBC). However, zinc (Zn) remained the most limiting element for certification. Overall, the findings demonstrate that the co-pyrolysis of BSs with agroforestry biomasses is an effective and sustainable strategy for generating stable and environmentally safe biochars, suitable for use as soil amendments and for the sustainable valorisation of BSs.

Keywords: biochar; co-pyrolysis; urban biosolids; rice husk; pruning waste; agricultural application

Academic Editor: James McGregor

Received: 19 November 2025
Revised: 18 December 2025
Accepted: 24 December 2025
Published: 8 January 2026

1. Introduction

The management of biosolids (BSs), a by-product produced in large quantities by wastewater treatment plants, presents an environmental challenge due to its potential toxicity and the need to develop sustainable alternatives for its final disposal [1,2]. Among the most extensively researched options, pyrolysis has emerged as a promising strategy for converting this waste into biochar, a material with properties of significant interest in both agricultural and environmental applications.

Biochar derived from BSs offers several advantages, including its high carbon content, nutrient contribution, and elevated cation exchange capacity. These characteristics enhance its potential for improving soil quality and removing contaminants from wastewater [3,4]. However, biochar produced from BSs also has notable limitations, such as high ash content, low calorific value, an underdeveloped porous structure, and a limited number of surface functional groups [1,2]. Furthermore, while pyrolysis contributes to the partial immobilisation of heavy metals (HMs) by converting them into more stable fractions, this process also increases their concentration in biochar, which limits its applicability in large-scale agriculture and environmental contexts [5].

To address these limitations, co-pyrolysis of BSs with supplementary bio-based feedstocks has emerged as a promising strategy to enhance biochar properties while mitigating its toxicity [6,7]. This approach entails the simultaneous conversion of two or more raw materials within a single pyrolysis system. Among the various options, the incorporation of additional biomass has been extensively investigated due to its low cost, minimal energy requirements, and its capacity to improve both the porous structure and the overall quality of the resulting biochar [1,8].

Biomass employed in co-pyrolysis can be classified into six principal categories: forest residues, agricultural residues, food processing by-products, recycled materials, anaerobic digestion digestates, and other diverse sources [6]. Among these, agricultural residues are the most frequently utilised co-substrates. A prominent example is the co-pyrolysis of BSs with cotton stalks, which has been shown to substantially enhance carbon content, aromaticity, and porosity, thereby increasing the adsorption capacity for HMs and organic contaminants [5]. Likewise, the incorporation of RH has proven effective in stabilising bioavailable HMs into less mobile fractions, consequently reducing the toxicity of the resulting biochar [9]. Nevertheless, the inherent variability in biomass composition necessitates further investigation to ascertain the reproducibility of these outcomes across different geographical and environmental contexts.

The characterisation of biochar encompasses its physical, chemical, and biological attributes, which collectively determine its applicability and performance. At present, two international frameworks govern its certification and commercial utilisation: the EBC and the IBI. Both frameworks provide comprehensive guidelines for production and evaluation, emphasising the critical control of HMs, including cadmium (Cd), chromium (Cr), copper (Cu), lead (Pb), nickel (Ni), and zinc (Zn), which must be strictly regulated when biochar is intended for agricultural applications [10,11].

In this context, BSs are regarded as a viable feedstock for biochar production; however, their application in agriculture is constrained by the presence of HMs. Co-pyrolysis with agroforestry-derived biomass has emerged as a promising strategy to stabilise these contaminants. Consequently, it is imperative to evaluate the extent to which this approach enhances the properties defined by international certification standards and whether it enables the safe utilisation of biochar in agricultural soils.

In Mexico, research on biochar derived from BSs remains at an early stage, and investigations into co-pyrolysis are virtually absent. This situation underscores the urgent need to generate knowledge that provides sustainable solutions for the management of such waste.

Although several international studies have explored co-pyrolysis as a strategy to enhance biosolid-based biochars, there is still limited understanding of how different co-substrates and their mass proportions influence the physicochemical transformations and heavy metal behaviour most relevant to compliance with international certification frameworks such as IBI and EBC. By evaluating the co-pyrolysis of BSs with RH and PW at multiple temperatures and mass ratios, the present study addresses this gap and provides insight into how biomass selection and proportion modulate carbon stability, mineral dynamics, and the key properties considered in international standards. This contribution aims to advance current co-pyrolysis research by offering comparative evidence that informs the design and evaluation of biosolid-derived biochars.

2. Materials and Methods

2.1. Collection and Preparation of Biomass

2.1.1. Biosolids (BSs)

The BSs were collected in October 2023 from the urban wastewater treatment plant (PTARU) in Celaya, Guanajuato, Mexico (100°51′38″ W, 20°30′46″ N). These BSs originated as by-products of the aerobic digestion of urban wastewater via secondary biological treatment. They exhibited a semi-solid consistency, with an average moisture content of 85% by mass, resulting from chemical stabilisation using a cationic polymer, followed by dewatering of the solids through a filter press system. Approximately 150 kg of BSs (wet basis) were collected at the filter press outlets and transported to the laboratory in plastic containers. Upon collection, the samples were air-dried for 30 days, after which they were manually ground and sieved through a 2 mm mesh. The sieved material was then stored in resealable transparent plastic bags and kept under refrigeration until use in subsequent analyses.

2.1.2. Pruning Waste (PW)

The PW was provided by the General Directorate of Environment (DGMA) of the Municipality of Celaya, Mexico, and was collected in October 2023 at the Bicentennial Linear Park (PLB) (100°47′2″ W, 20°30′25″ N). The PW, sourced from various logs, was shredded using a Bear Cat 3″ (10 HP) chipper to produce wood chips measuring 3–5 cm in length and approximately 0.5 cm in thickness. The resulting chips were transported to the laboratory, where they were air-dried. Subsequently, the dried material was ground using a 1000 W Natural Bullet processor and sieved through a 2 mm mesh. The final samples were stored in sealed plastic containers and kept at room temperature until further analyses.

2.1.3. Rice Husk (RH)

The RH employed in this study was commercially obtained from BIOJAL®(Guadalajara, Mexico). The material was ground using a 1000 W Natural Bullet processor (Zhongshan, China) and subsequently sieved through a 2 mm mesh. The resulting fractions were stored in sealed plastic containers and maintained at room temperature until further analyses were conducted.

2.2. Production of Biochars via Pyrolysis and Co-Pyrolysis

Preparation of Biomass for Pyrolysis and Co-Pyrolysis

The biomasses selected for pyrolysis comprised BS, PW, and RH. For co-pyrolysis, these biomasses were combined according to specific mass ratios (w/w). The biomass and mixtures in mass proportions used in the production of biochars are summarised in Table 1.

Table 1. Biomass Materials Utilised for Biochar Production via Pyrolysis and Co-Pyrolysis.

Biomass		Identification Code
Biosolids (BSs)		BS
Rice husk (RH)		RH
Pruning waste (PW)		PW
Biomass	**Mass Ratio (*w*/*w*)**	**Identification Code**
BS/RH	1:1	BS/RH (1:1)
	2:1	BS/RH (2:1)
	1:2	BS/RH (1:2)
BS/PW	1:1	BS/PW (1:1)
	2:1	BS/PW (2:1)
	1:2	BS/PW (1:2)
BS/RH/PW	1:1:1	BS/RH/PW (1:1:1)

2.3. Pyrolysis Reactor

A pilot-scale fixed-bed reactor was employed for biochar production. Before each experimental run, nitrogen (N_2) was injected into the reactor at a flow rate of 50 mL min^{-1} for 5 min to eliminate any trace of air and ensure an oxygen-free atmosphere during operation. Reactor temperature was monitored using a K-type thermocouple connected to an Arduino UNO board (Scarmagno, Italy) through a MAX6675 module (Sunnyvale, CA, USA), providing precise and continuous temperature acquisition. Heating was supplied by a 3500 W, 220 VAC clamp resistor controlled via an Autonics SPC1-50 power controller (Seoul, Republic of Korea). The thermal trajectory of the system was regulated by a first-order Smith predictive control scheme with a 225 s delay implemented in MATLAB® 2021a, ensuring accurate temperature tracking and operational stability throughout the process [12]. After the heating stage, the reactor was allowed to cool to ambient temperature by natural convection, after which the biochar was recovered for subsequent characterisation.

2.4. Process Conditions for Biochar Production

For biochar production, 50 g of each biomass, according to the proportions detailed in Table 1, were accurately weighed and introduced into the reactor. The pyrolysis process was conducted at three target temperatures: 300 °C, 400 °C, and 500 °C, employing a heating rate of 20 °C min^{-1} and a residence time of 20 min. These operating conditions were selected to represent a typical slow pyrolysis regime, commonly applied in biochar production for soil applications, allowing the evaluation of progressive thermal decomposition, carbon structural development, and stabilisation processes in biosolids and co-pyrolysed biomass. Upon completion of the thermal treatment, the samples were cooled under natural convection until the reactor's internal temperature reached 50 °C, minimising post-pyrolysis oxidation and preserving the physicochemical properties of the resulting biochars. The biochars were subsequently weighed and stored in airtight plastic containers for further analyses. Biochar yield was calculated using Equation (1), following the methodology described by [13]

$$\%Y = m_1/m_2 \times 100, \quad (1)$$

where m_1 is the weight of biochar and m_2 is the weight of biomass sample.

2.5. Characterisation of Biomasses and Biochars

2.5.1. Physicochemical Parameters

Proximate Analysis of Biomasses and Biochars (Moisture and Ash Content)

The proximate analysis of the biomasses involved the determination of moisture and ash contents in accordance with established ASTM standards, including the Standard Test Method for Ash in Wood (n.d.), the Standard Test Method for Moisture Analysis of Particulate Wood Fuels (n.d.), and the Standard Test Method for Volatile Matter in the Analysis of Particulate Wood Fuels (n.d.) [14–16].

Approximately 0.5 g of biochar from each treatment was placed into individual crucibles, which were subsequently heated in a RIOSA H-3 oven, model H-33 (Mexico City, Mexico) at 105 °C for 2 h. Upon completion, the crucibles were transferred to a desiccator for 1 h to allow cooling to ambient temperature, after which their weights were recorded. For the determination of ash content, the dried samples were then introduced into a FE-LISA muffle furnace, model FE-360 (Zapopan, Mexico), and maintained at 750 °C for 6 h. Following this high-temperature treatment, the samples were again cooled in a desiccator for 1 h prior to the final weight measurements. Prior to analysis, all biochar samples were thoroughly homogenised to ensure representativeness, and each determination was performed in triplicate. The reported values correspond to mean ± standard deviation, obtained using an analytical balance with a precision of ±0.0001 g, which explains the low variability observed in moisture and ash content measurements.

Elemental Analysis of Biomasses and Biochars

Elemental analysis of the biomasses and biochars was conducted using a Thermo Scientific FlashSmart elemental analyser (Waltham, MA, USA), following the procedure described by [17], to quantify the contents of carbon, hydrogen, nitrogen, and sulphur (C, H, N, and S). The oxygen content was subsequently calculated by difference, according to the methodology reported by [18].

Hydrogen Potential (pH) and Electrical Conductivity (EC) of Biochars

To assess the pH and EC of the biochars, 20 mL of deionised water was added to 1 g of each biochar sample, and the mixture was vortexed for 90 min. The supernatant was then carefully decanted for the measurement of both parameters, following the procedure outlined by [19]. The pH was measured using a Denver Instrument UB-10 potentiometer (Denver, CO, USA), while EC was determined with a Horiba Laqua Model F-74BW conductivity meter (Kyoto, Japan).

Particle Size Analysis of Biochars

The surface area, pore size, and pore volume of the biochars were determined using the BET (Brunauer, Emmett, and Teller) method, based on nitrogen adsorption isotherms. This approach quantifies the multilayer adsorption capacity at varying partial pressures of nitrogen, following the methodology described by [17]. Analyses were performed using a Quantachrome Nova BET analyser, model 4200 E (Hidalgo, Mexico), with nitrogen as the adsorbate at 77 K.

Morphological and Spectroscopic Analysis of Biomasses and Biochars

The surface organic functional groups of both the biomasses and biochars were characterised using attenuated total reflectance Fourier transform infrared spectroscopy (ATR-FTIR) with a Thermo Nicolet IS10 spectrophotometer (Waltham, MA, USA). For pellet preparation, 0.05 g of the crushed and homogenised sample was thoroughly mixed with 0.1 g of KBr and pressed using a hydraulic press. The FTIR absorbance spectra were ac-

quired over a wavenumber range of 4000–400 cm^{-1}, at a resolution of 4 cm^{-1}, in accordance with the procedure described by [20].

To investigate the surface morphology, pore structure, and both structural and elemental modifications, scanning electron microscopy (SEM) was employed, exploiting the interaction between the electron beam and the biochars [17]. Additionally, energy dispersive spectroscopy (EDS) was utilised to determine the elemental composition at the biochar surface, leveraging the characteristic energies of X-ray photons emitted by each element [17]. These analyses were conducted using a JSM-7401F field emission microscope (Tokio, Japan) equipped with an EDS system for X-ray dispersion and fluorescence spectrometry.

2.6. Quantification of Metals and Metalloids

The concentrations of metals and metalloids (Al, Cd, Cr, Cu, Fe, K, Mg, Ni, Pb, and Zn) in the produced biochars were determined using an acid digestion procedure. For each biochar sample, 0.3 g was accurately weighed, and a mixture of HNO_3, H_2O_2, and HCl was added. The samples were subsequently heated on a Thermo Scientific Cimarec+ Ceramic Stirrer S88857100 (St. Louis, MO, USA) heating and stirring unit at 110 °C [5]. Upon completion of the digestion, each sample was filtered through Whatman No. 40 filter paper and adjusted to a final volume of 50 mL. The elemental concentrations were then determined by inductively coupled plasma optical emission spectrometry (ICP-OES) using a Thermo Scientific iCAP 7400 spectrometer (Montevideo, Uruguay) [21].

2.7. Germination Percentage

The germination percentage was evaluated using a methodology adapted from that described by [22]. Agricultural soil was collected from the community of Arreguín de Abajo, within the municipality of Celaya, Guanajuato, Mexico (20°28′27.0″ N, 100°49′51.2″ W). The soil was air-dried and sieved through a 2 mm mesh to ensure homogenisation. Soil moisture content was determined by drying a 2 g subsample in a RIOSA H-3 oven, model H-33 (Mexico City, Mexico), at 105 °C for 24 h, following the procedures outlined by [23,24]. Soil pH was measured according to [25] using a 1:2.5 (w/v) soil-to-water ratio with a Denver Instrument UB-10 potentiometer (Arvada, CO, USA), while EC was determined following the method of [26] using a 1:5 (w/v) soil-to-water ratio with a Horiba Laqua model F-74 conductometer (Kyoto, Japan).

Maize was selected as the model plant for germination and growth experiments due to its agronomic significance in Mexico. Grano GV forage maize seeds, commercially obtained from GOLDEN VEGETABLE SEEDS(Guadalajara, Mexico), were washed with running water and soap to remove residual fungicide, followed by immersion in running water for 24 h. Each biochar was incorporated into 240 g of soil at a uniform rate of 2% on a dry weight basis. The resulting mixtures were thoroughly homogenised, and 40 g portions were transferred to individual wells of germination trays, with six subsamples prepared per treatment. The allocation of wells and subsequent analyses were conducted in a completely randomised manner. Control units consisted of soil without biochar, and all treatments were maintained at the same biochar application rate of 2% dry weight [19].

Prior to sowing, the germination trays with individual wells were incubated under greenhouse conditions for 20 days, maintaining a photoperiod of 16 h of light and 8 h of darkness, with day/night temperatures of approximately 25 °C/15 °C. Irrigation was performed manually to ensure consistent moisture: initially, the trays were weighed and flooded with running water, and excess water was removed the following day. Trays were then reweighed and additional water added to achieve a target soil moisture content of 70%. After the 20-day incubation period, a single maize seed was sown in each well, resulting in

a total of 150 seeds across all treatments, including controls. Germination was monitored daily from day 2 to day 12 post-sowing.

2.8. Plant Growth Test

As outlined in the previous section, each maize seed was sown individually in the pre-incubated germination trays. Twelve days post-sowing, the maize plants were harvested. The aerial and root tissues were measured and weighed to determine their fresh biomass. Subsequently, the plants were transferred to paper bags and oven-dried at 70 °C for 72 h, after which their dry weight was recorded. The collected data were then used to calculate the relative seed germination rate (RSGR), relative root growth (RRG), and germination index (GI), following the methodology described by [27].

$$\text{RSGR} = \text{Sc}/\text{Ss} \times 100, \tag{2}$$

$$\text{RRG} = \text{Rs}/\text{Rc} \times 100 \tag{3}$$

$$\text{GI} = \text{RSGR}/\text{RRG} \times 100 \tag{4}$$

where Ss represents the number of seeds germinated in the sample, Sc denotes the number of seeds germinated in the control, Rs corresponds to the average root length in the sample, and Rc refers to the average root length in the control.

2.9. Statistical Analysis

Statistical analyses of the maize plant growth data were conducted using OriginPro, version 2024. Differences between the means of the measured parameters were assessed via analysis of variance (ANOVA), followed by Tukey's post hoc test at a significance level of $p < 0.05$.

For the evaluation of the 22 biochar characterisation parameters, principal component analysis (PCA) was performed in OriginPro, version 2024, to identify the primary factors contributing to the observed differences among treatments. This multivariate analysis involved factorising the standardised variance-covariance matrix and extracting its eigenvalues and eigenvectors to capture the overall variability across all experimental units and treatment combinations. The resulting reduced Euclidean planes facilitated comparison of the mean projection distances of each experimental unit along the first two principal components, corresponding to the eigenvectors with the largest eigenvalues [28–30].

3. Results and Discussion

3.1. Physical and Elemental Properties

3.1.1. Biomass Characterisation

The physicochemical properties of the biomasses are summarised in Table 2. Regarding elemental composition, the carbon (C) content was 34.18% in BS, 29.93% in RH, and 42.17% in PW, with PW exhibiting the highest C concentration and RH the lowest. N contents were 6.30% in BS, 1.04% in RH, and 2.18% in PW, with BS showing the highest N content. Sulphur (S) was detected only in BS, at a concentration of 0.45%. These observations align with the high fraction of organic matter in BS, primarily composed of hydrocarbons, amino acids, and lipids, alongside a relatively low proportion of lignin and cellulose [3].

Table 2. Biomasses Utilised for Biochar Production via Pyrolysis and Co-pyrolysis.

Items	BS	RH	PW
Moisture %	11.01 ± 0.39	6.49 ± 0.34	7.08 ± 0.15
Ash %	27.31 ± 0.16	22.32 ± 0.23	6.69 ± 0.10
C %	34.178	29.93	42.167
N %	6.304	1.045	2.179
S %	0.452	N/D	N/D

With respect to ash content, BS exhibited the highest value (27.31 ± 0.17%), followed by RH (22.32 ± 0.24%) and PW (6.69 ± 0.10%). This parameter is particularly significant, as the ash remains in the biochar after pyrolysis and can substantially influence critical properties such as pH and material yield [31].

3.1.2. Characterisation of Biochar

The elemental and proximate analyses of the biochars produced through pyrolysis and co-pyrolysis at various temperatures are presented in Table 3, and Figure 1. The parameters evaluated included: moisture content, ash content, pH, EC, yield, elemental composition (C, H, N, O, and S), and the H/C ratio.

Table 3. Proximate Analysis of Biochars Produced by Pyrolysis and Co-Pyrolysis at 300 °C.

Biochar 300 °C	**Proximate Analysis of Biochars**			
	Moisture %	**Ash %**	**pH**	**EC (mS·m^{-1})**
BS	0.93 ± 0.079	40.6 ± 1.030	5.75 ± 0.063	32.2 ± 4.76
BS/RH 1:1	0.93 ± 0.023	40.6 ± 0.040	5.12 ± 0.007	38.9 ± 0.29
BS/RH 1:2	0.92 ± 0.070	38.1 ± 0.201	5.54 ± 0.389	48 ± 0.10
BS/RH 2:1	1.09 ± 0.027	39.4 ± 0.218	5.30 ± 0.099	40.6 ± 0.33
BS/PW 1:1	2.02 ± 0.968	25.5 ± 0.727	4.85 ± 0.028	86 ± 4.39
BS/PW 1:2	1.25 ± 0.147	22.0 ± 0.151	6.02 ± 0.028	55 ± 7.45
BS/PW 2:1	1.08 ± 0.147	32.6 ± 0.925	5.64 ± 0.056	42.7 ± 4.14
BS/RH/PW 1:1:1	0.95 ± 0.020	31.1 ± 0.242	5.70 ± 0.049	49 ± 7.01
Biochar 400 °C	**Moisture %**	**Ash %**	**pH**	**EC (mS·m^{-1})**
BS	0.782 ± 0.121	52.0 ± 0.095	6.47 ± 0.035	16.5 ± 2.92
BS/RH 1:1	0.897 ± 0.015	47.8 ± 0.096	6.25 ± 0.007	27.7 ± 0.63
BS/RH 1:2	0.859 ± 0.114	51.1 ± 0.436	7.55 ± 0.148	24.9 ± 3.59
BS/RH 2:1	0.653 ± 0.119	49.3 ± 0.427	6.13 ± 0.007	24.9 ± 6.48
BS/PW 1:1	0.984 ± 0.036	33.2 ± 0.961	5.96 ± 0.063	26.8 ± 2.64
BS/PW 1:2	0.874 ± 0.283	27.7 ± 0.208	6.59 ± 0.056	34.6 ± 0.29
BS/PW 2:1	0.811 ± 0.002	42.3 ± 0.314	6.32 ± 0.127	25.8 ± 3.10
BS/RH/PW 1:1:1	1.19 ± 0.110	39.5 ± 0.116	7.08 ± 0.021	32.9 ± 2.13
Biochar 500 °C	**Moisture %**	**Ash %**	**pH**	**EC (mS·m^{-1})**
BS	0.585 ± 0.067	60.4 ± 0.724	6.56 ± 0.084	11.8 ± 0.20
BS/RH 1:1	0.501 ± 0.074	55.0 ± 0.083	7.31 ± 0.212	23.5 ± 3.39
BS/RH 1:2	0.744 ± 0.016	54.0 ± 0.458	7.91 ± 0.077	31.7 ± 4.25
BS/RH 2:1	0.586 ± 0.153	56.6 ± 0.583	6.95 ± 0.099	22.5 ± 1.63
BS/PW 1:1	0.762 ± 0.008	45.5 ± 0.212	7.67 ± 0.063	20.3 ± 3.39
BS/PW 1:2	0.389 ± 0.437	37.0 ± 0.263	7.87 ± 0.014	20.7 ± 2.69
BS/PW 2:1	0.722 ± 0.013	48.2 ± 0.269	7.71 ± 0.042	18.4 ± 0.15
BS/RH/PW 1:1:1	0.197 ± 0.024	45.7 ± 0.115	7.95 ± 0.000	22.7 ± 3.06

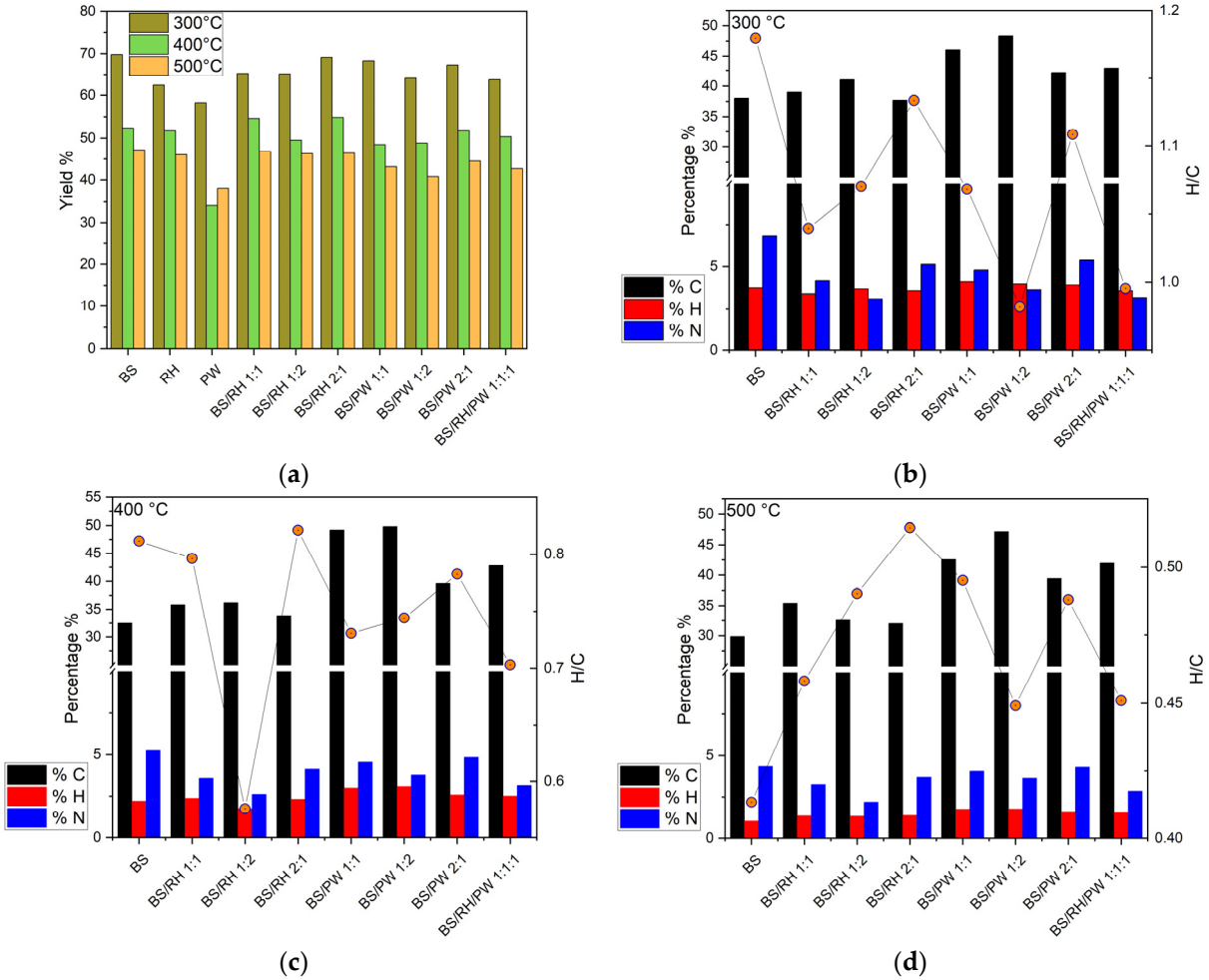

Figure 1. Characterization of biochars, (**a**) Yield of biochars at 300 °C, 400 °C and 500 °C, (**b**) Percentage of Carbon, hydrogen, nitrogen and H/C ratio of biochars at 300 °C, (**c**) Percentage of Carbon, hydrogen, nitrogen and H/C ratio of biochars at 400 °C (**d**) Percentage of Carbon, hydrogen, nitrogen and H/C ratio of biochars at 500 °C. H/C ratio of biochars in red dots.

Biochar Moisture Percentage

The moisture content of the biochar decreased as the pyrolysis temperature increased. At 300 °C, the values ranged from 2.02 ± 0.97% (BS/PW 1:1) to 0.92 ± 0.07% (BS/RH 1:2). At 400 °C, the range was from 1.19 ± 0.11% (BS/RH/PW 1:1:1) to 0.65 ± 0.12% (BS/RH 2:1), while at 500 °C, the values ranged from 0.72 ± 0.01% (BS/PW 2:1) to 0.20 ± 0.02% (BS/RH/PW 1:1:1) (see Table 3). In general, BS/PW biochar exhibited the highest moisture content, whereas BS/RH biochar displayed the lowest.

Biochar Ash Content

The ash content in biochar increased with the pyrolysis temperature. At 300 °C, values ranged from 40.64 ± 1.03% (BS) to 21.10 ± 0.15% (BS/PW 1:2). At 400 °C, the range was from 51.96 ± 0.09% (BS) to 27.69 ± 0.21% (BS/PW 1:2), while at 500 °C, values ranged from 60.44 ± 0.72% (BS) to 36.95 ± 0.26% (BS/PW 1:2) (see Table 3). At all three temperature levels, biochar produced exclusively from BSs exhibited the highest ash content. In contrast, the inclusion of PW in co-pyrolysis (BS/PW ratio 1:2) resulted in a reduction in ash content of 54.12%, 53.30%, and 61.13% compared to the maximum values observed for BS at 300, 400, and 500 °C, respectively.

Yang et al. [32] evaluated the co-pyrolysis of municipal sewage sludge (MSS) with sawdust (SD) at various ratios and temperatures. They reported ash contents in the pure

MSS biochars of 60.7%, 65.6%, and 68.5% at 300, 400, and 500 °C, respectively. In contrast, the BS-derived biochars obtained in the current study demonstrated lower ash values (40.64%, 51.96%, and 60.44% at the same corresponding temperatures). When considering co-pyrolysis, Yang et al. [32] reported ash contents of 41%, 43.7%, and 44.6% for the MSS + SD (5:5) mixture, whereas the BS/PW (1:1) biochars in this work achieved values of 25.48%, 33.21%, and 45.53%. This indicates similarity only at the highest temperature (500 °C), with significantly lower percentages observed at both 300 °C and 400 °C. Both studies consistently observed a progressive increase in ash content with rising pyrolysis temperature. Nevertheless, the values obtained in the current investigation were generally lower than those previously reported. These distinctions can primarily be attributed to differences in the ash content of the source biomass and their specific harvesting conditions [31].

These differences in ash content can be explained by the underlying pyrolytic behavior of biosolids and their interactions with lignocellulosic co-substrates. As temperature increases, the progressive loss of volatiles concentrates thermally stable inorganic fractions such as silicates, phosphates and metal oxides, leading to higher ash proportions in BS-derived biochars. Co-pyrolysis with PW, however, dilutes the mineral load of BSs and modifies mineral–organic transformations, resulting in consistently lower ash yields than BSs alone. Similar synergistic effects have been reported in sludge–biomass systems, where lignocellulosic volatiles partially inhibit mineral decomposition at intermediate temperatures and promote phase restructuring at higher temperatures, ultimately influencing ash evolution and composition [8,21,33].

Hydrogen Potential (pH) of Biochars

The pH of the biochars progressively increased with the pyrolysis temperature. At 300 °C, values ranged from 6.02 ± 0.03 (BS/PW 1:2) to 5.11 ± 0.01 (BS/RH 1:1), remaining within a slightly acidic range (see Table 3). At this temperature, the addition of RH in any proportion resulted in a reduction in pH compared to pure BS biochar, while the inclusion of PW in a higher proportion (BS/PW 1:2) caused an increase in pH.

At 400 °C, the pH values of the biochars ranged from 7.56 ± 0.15 (BS/RH 1:2) to 5.97 ± 0.06 (BS/PW 1:1) (see Table 3). Although some biochars remained slightly acidic, particularly those generated with PW, mixtures containing a higher proportion of RH (BS/RH 1:2) approached neutral pH values.

At 500 °C, pH values ranged from 7.95 ± 0.18 (BS/RH/PW 1:1:1) to 6.56 ± 0.08 (BS) (see Table 3). In this temperature range, most biochars exhibited alkaline characteristics, with pure BS biochar being the only exception, remaining slightly acidic. Overall, the addition of RH or PW in higher proportions during pyrolysis generally facilitated an increase in pH.

Previous studies have demonstrated that the pH of biochars varies markedly depending on the feedstock type used in their production. Reference [34] reported that biochars derived from BSs exhibit acidic characteristics when subjected to low-temperature pyrolysis (300–400 °C). Conversely, refs. [21,35] observed that biochars produced from activated sludge (AS) tend to be neutral to slightly alkaline, with pH values ranging from 6.2 to 9.3, depending on the pyrolysis temperature applied.

The results of this study, in which biochars derived from BSs exhibited pH values of 5.8, 6.5, and 6.6, fall within the acidic range and are consistent with the findings reported by [34]. However, these values contrast with the higher pH levels observed for biochars produced from AS, as noted by [21,35]. These discrepancies indicate that the feedstock origin (BS vs. AS) plays a determinant role in defining the final pH of the biochar. Consequently, the

selection of the base material directly influences the acidity or alkalinity of the product, which in turn affects its suitability for different agricultural and environmental applications.

Regarding co-pyrolysis with RH, ref. [13] reported that the co-pyrolysis of AS with rice straw (RS) in a 1:1 ratio produced biochars with pH values of 5.3, 6.4, and 7.0 at 300, 400, and 500 °C, respectively, exhibiting a trend towards neutrality. Similarly, ref. [9] indicated that a sewage sludge/rice husk (SS/RH, 50/50) mixture generated biochars with pH values of 7.13 ± 0.34, 7.28 ± 0.32, and 9.22 ± 0.39 at the same temperatures, reflecting a predominantly alkaline behaviour. In the present work, BS/RH (1:1) biochars displayed pH values of 5.11 ± 0.01, 6.26 ± 0.01, and 7.31 ± 0.21 at 300, 400, and 500 °C, respectively, results that are more closely aligned with those reported by [13].

Huang et al. [13] reported that the co-pyrolysis of AS with SD in a 1:1 ratio yielded biochars with pH values of 6.0, 6.8, and 7.4 at 300, 400, and 500 °C, respectively, exhibiting a progressive shift towards neutrality with increasing temperature. In contrast, ref. [21] found that the co-pyrolysis of SS with cotton stalks (CS) in the same proportion produced biochars with markedly more alkaline pH values of 9.2, 10.1, and 10.5 under identical temperature conditions. In the present study, biochars derived from BS and PW (BS/PW, 1:1) exhibited pH values of 4.9, 5.9, and 7.7 at 300, 400 and 500 °C, respectively, demonstrating a comparable upward trend in pH with increasing pyrolysis temperature.

These results indicate that, although the observed increase in pH with rising pyrolysis temperature is consistent with trends reported in the literature, the pH values obtained for BS/PW biochars are lower than those reported by [21], and more closely aligned with those observed by [13], particularly at 500 °C.

Comparisons with previous studies on the co-pyrolysis of BSs with RH and PW reveal notable differences in pH values, which can be primarily attributed to the intrinsic characteristics of the feedstocks employed. In the present study, it was observed that at 300 and 400 °C, biochars derived from BSs co-pyrolysed with RH and PW exhibited acidic pH values, whereas at 500 °C they became alkaline. This behaviour is of particular relevance, as pH is one of the most influential chemical properties governing the agronomic suitability of biochars as soil amendments [36].

Specifically, the biochars produced in this work display a pH range broad enough to enable their application in both acidic and alkaline soils [3]. In acidic soils, the use of alkaline biochars can raise soil pH, induce a liming effect, and enhance the bioavailability of basic nutrients [37–43]. Conversely, in alkaline soils, the addition of acidic or near-neutral biochars may cause a slight reduction in pH, favouring the solubility of nutrients such as phosphorus (P) and trace elements [37,44]. However, such reductions are typically minor and exert limited influence on overall nutrient availability [37,45]. Given that most biochars reported in the literature are intrinsically alkaline, their incorporation into alkaline soils generally results in negligible changes in soil chemical properties [37].

The progressive increase in pH with temperature can be attributed to the thermally induced decomposition of acidic surface groups and the concurrent concentration or formation of alkaline mineral species such as carbonates, oxides and silicates. During co-pyrolysis, lignocellulosic volatiles interact with BS-derived minerals, influencing the release, transformation and retention of basic cations (Ca, Mg, K, Na), which contributes to the distinct pH patterns observed among RH- and PW-based mixtures. Previous studies on sludge–biomass systems have reported similar synergistic effects, where the mineral composition of the co-substrate and its ash chemistry modulate the extent of deacidification and mineral alkalisation during thermal treatment. These mechanisms help explain the lower pH values in PW blends at moderate temperatures and the stronger alkalinisation observed in RH mixtures at 500 °C [8,33,46].

Electrical Conductivity (EC) of Biochars

According to [45], biochar intended for agricultural applications should exhibit high EC, as this parameter reflects the presence of inorganic salts such as potassium (K), sodium (Na), calcium (Ca), and magnesium (Mg). These salts constitute essential macronutrients that are released into the soil upon biochar incorporation. Moreover, it has been reported that the combination of high EC with a neutral to slightly alkaline pH (7–10) is advantageous for agronomic use, since such conditions enhance nutrient availability and promote optimal plant growth following soil application [47,48].

The EC of the biochars produced in this study decreased progressively with increasing pyrolysis temperature. At 300 °C, EC values ranged from 86.00 ± 0.04 mS m^{-1} for BS/PW (1:1) biochar to 32.25 ± 0.05 mS m^{-1} for BS biochar. At 400 °C, the EC ranged from 34.60 ± 0.003 mS m^{-1} for BS/PW (1:2) to 16.55 ± 0.03 mS m^{-1} for BS, whereas at 500 °C, values ranged from 31.68 ± 0.04 mS m^{-1} for BS/RH (1:2) to 11.84 ± 0.002 mS m^{-1} for BS (see Table 3).

In contrast to the pH behaviour, EC exhibited a declining trend with increasing pyrolysis temperature, suggesting that soluble inorganic ions were transferred from the solid phase (biochar) to the liquid phase (bio-oil) during the pyrolysis process [49,50].

During BS pyrolysis, the EC values obtained in this study were 32.25 ± 0.05, 16.55 ± 0.03, and 11.83 ± 0.00 mS m^{-1} at 300, 400 and 500 °C, respectively, demonstrating a clear decreasing trend with increasing temperature. Similarly, ref. [35] reported a decline in EC for biochars derived from AS, although their values were considerably higher (330, 40, and 50 mS m^{-1} at 300, 400 and 500 °C, respectively). In contrast, ref. [49] observed an increase in EC with temperature (50, 80, and 70 mS m^{-1}), suggesting variability in pyrolytic behaviour across studies.

These discrepancies underscore the lack of consistency in EC values reported in the literature, likely arising from differences in feedstock composition, mineral content, and pyrolysis conditions. Nonetheless, the results of the present work are consistent with the decreasing trend reported by [35], albeit with lower absolute EC values.

The co-pyrolysis of BS with RH and PW resulted in higher EC values compared with the individual pyrolysis of BS alone, while maintaining the overall decreasing trend with increasing temperature across all mass ratios evaluated. In the case of co-pyrolysis with RH, the highest EC values were observed for the 1:2 ratio, reaching 48.00, 25.00, and 31.68 mS m^{-1} at 300, 400 and 500 °C, respectively. Similarly, for co-pyrolysis with PW, the same ratio yielded EC values of 55.01, 34.59, and 20.74 mS m^{-1} at the corresponding temperatures.

When comparing both treatments, it was evident that PW-assisted pyrolysis produced higher EC values than those obtained with RH at 300 and 400 °C, whereas at 500 °C the values were comparable. This observation suggests a greater retention of soluble inorganic ions in the BS/PW-derived biochar at lower pyrolysis temperatures.

Comparison with previous studies is somewhat constrained, as only a limited number of reports include EC measurements. Nevertheless, ref. [13] documented considerably lower EC values for the co-pyrolysis of AS with RS and SD, ranging from 19–4.5 mS m^{-1} and 11–6.5 mS m^{-1}, respectively, between 300 and 500 °C. In contrast, in the present study, the equivalent treatments—BS/RH (1:1) and BS/PW (1:1)—exhibited higher EC values, ranging from 38.89–23.53 mS m^{-1} and 86.00–20.30 mS m^{-1}, respectively. Despite these quantitative differences, both the findings of [13] and those of the present work demonstrate a consistent trend of decreasing EC with increasing pyrolysis temperature.

Overall, the relatively high EC values observed in the co-pyrolysis of BSs with RH and PW indicate an enhanced release of mineral nutrients, highlighting the potential agronomic benefits of these biochars. Nonetheless, excessive salt accumulation may adversely affect

seed germination and plant development, particularly in arid or poorly drained soils where leaching is limited [36]. Consequently, further validation through germination bioassays and soil–biochar interaction studies is warranted to ensure that the application of these materials promotes soil fertility without compromising crop establishment or growth.

The decreasing EC with rising temperature can be attributed to the progressive redistribution of alkali and alkaline-earth ions during pyrolysis. As organic matter decomposes, part of the soluble mineral fraction volatilises, migrates into the bio-oil phase, or becomes incorporated into more stable mineral structures, reducing its availability in the solid char. Co-pyrolysis modifies these pathways because lignocellulosic volatiles interact with BS-derived minerals, influencing ion mobility and favouring higher EC values in BS/RH and BS/PW mixtures compared with BS alone. Similar synergistic effects have been reported in sludge–biomass systems, where biomass components modulate mineral transformations and the retention of soluble salts during thermal conversion [8,33,46].

Biochar Yields

The yield of biochar obtained through pyrolysis depends on both the operational conditions and the inherent characteristics of the feedstock used [31]. This parameter is critical for assessing the conversion efficiency and economic viability of the process, as it indicates the proportion of solid product generated under specific thermal conditions.

In the present study, the biochar yields obtained at 300 °C ranged from 69.79% (BS) to 63.74% (BS/RH/PW 1:1:1). At 400 °C, the values varied from 54.82% (BS/RH 2:1) to 48.42% (BS/PW 1:1), whereas at 500 °C, yields ranged from 47.13% (BS) to 40.80% (BS/PW 2:1). Overall, an inverse relationship between temperature and yield was observed, with the most pronounced reduction occurring at 500 °C (see Figure 1a). This declining trend with increasing temperature has been widely reported in the literature [5,9,13,21,35,49,50] and is generally attributed to a higher degree of biomass decomposition, involving both primary breakdown of organic constituents and secondary reactions of the solid residue. These processes enhance the formation of liquid and gaseous fractions, thereby reducing the mass of the solid biochar produced [13,50,51].

During BS pyrolysis, the biochar yields were 69.79%, 52.28%, and 47.13% at 300, 400 and 500 °C, respectively, exhibiting a clear decline with increasing temperature, a trend that has been consistently reported in previous studies [3,34,51]. It is noteworthy that these yields were the highest among all treatments evaluated, which can be attributed to the high ash content of the BS. Such biomass typically produces greater solid residue yields, as the inorganic fraction resists thermal degradation and remains within the solid phase after pyrolysis [31].

The addition of RH and PW influenced the yield of co-pyrolysed biochars. Treatments with a higher proportion of BS—namely BS/RH 2:1 and BS/PW 2:1—achieved higher yields than those with lower BS content (BS/RH 1:2 and BS/PW 1:2), suggesting that the high ash content of BSs promotes solid mass retention during pyrolysis. This behaviour is consistent with previous studies, in which the incorporation of co-substrates in the co-pyrolysis of AS resulted in lower yields compared with the pyrolysis of pure AS. Such reductions have been attributed to the higher volatile matter and lower fixed carbon content typically present in lignocellulosic co-substrates [6,52,53]. As observed for BS pyrolysis, the co-pyrolysed biochars also exhibited a decline in yield with increasing temperature. Nevertheless, co-pyrolysis with RH tended to maintain higher yields than co-pyrolysis with PW, suggesting that RH acts as a more favourable co-substrate for maximising biochar production. In contrast, PW, owing to its greater content of volatile compounds, appears to reduce the efficiency of solid product formation.

Carbon Content

The carbon (C) content is one of the most important parameters in the characterisation of biochar, as it is directly associated with its chemical stability and suitability for soil applications [11]. This parameter depends on both the type of biomass employed and the pyrolysis temperature and typically increases relative to the raw biomass due to the progressive elimination of oxygen and hydrogen as volatile compounds during pyrolysis [31,52]. However, the effect of temperature on carbon content is not strictly linear and may vary depending on feedstock composition and co-pyrolysis conditions. Several studies have reported that intermediate temperatures can favour maximum carbon retention, whereas further increases in temperature may induce secondary devolatilisation or structural reorganisation, leading to a slight reduction in relative carbon content [8,33,46]. These dynamics influence the structural stability of biochar and its persistence in soil, which are key properties for carbon sequestration and soil quality enhancement applications. Consequently, as pyrolysis temperature rises, the relative carbon concentration increases, enhancing the structural stability of the biochar and extending its persistence in the soil. These properties are particularly advantageous for carbon sequestration and soil quality enhancement applications.

In this study, the carbon content of the biochars produced ranged from 48.36% to 37.71% at 300 °C, 49.82% to 33.87% at 400 °C, and 47.18% to 32.02% at 500 °C. The highest carbon concentrations were obtained from the co-pyrolysis of the BS/PW 1:2 mixture, whereas the lowest values corresponded to the BS/RH 2:1 mixture (see Figure 1a–c). Overall, the addition of co-substrates led to an increase in carbon content compared with the pyrolysis of BS alone, particularly in mixtures containing PW. These findings are consistent with those reported by [7], who observed a positive influence of carbon-rich co-substrates on the elemental composition of biochar. Moreover, the observed increase in carbon concentration aligns with the results of [31], who attributed this behaviour to the thermal decomposition of oxygen- and hydrogen-containing functional groups during pyrolysis, which enhances the relative carbon content in the solid residue.

The highest carbon content was observed in the biochars produced by the co-pyrolysis of the BS/PW 1:2 mixture across all temperature levels evaluated, whereas the lowest values corresponded to the BS/RH 2:1 mixture (see Figure 1b–d). This difference can be attributed to the nature of the feedstock used: lignocellulosic residues, such as PW, generally possess a higher intrinsic carbon concentration than agricultural or animal-derived biomasses, such as RH and BS, respectively [54–56]. This finding aligns with the classification of these substrates, which reflects their distinct carbon compositions and consequent influence on biochar yield and quality.

A similar trend was reported by [13], who evaluated the co-pyrolysis of SS with RS and SD in a 1:1 ratio. In their study, the carbon contents obtained for the SS/RS mixture were 35.8%, 33.7%, and 29.6% at 300, 400 and 500 °C, respectively—values that are comparable to those observed in the present work for the co-pyrolysis of the BS/RH 1:1 mixture, which yielded 39%, 35.84%, and 35.41% under the same temperature conditions. Similarly, the biochars obtained from the SS/SD mixture reported by [13] exhibited carbon contents of 42.5%, 47.2%, and 45.6%, values closely aligned with those achieved in this study for BS/PW 1:1 co-pyrolysis, which produced 46.05%, 49.21%, and 42.58%, respectively. These results reveal a consistent pattern concerning the influence of the lignocellulosic co-substrate type, both in previous studies and in the present work, thereby reinforcing the conclusion that the nature of the biomass employed in co-pyrolysis plays a decisive role in determining the final carbon content of the resulting biochar.

The differences in carbon content observed across mixtures and temperatures can be explained by the underlying pyrolytic pathways governing carbon retention during

thermal decomposition. As biomass is heated, the progressive cleavage of C–O, C–H and O–H functional groups promotes the formation of condensed aromatic domains, which become increasingly dominant at higher temperatures and contribute to the enrichment of carbon in the solid phase. Co-pyrolysis further modifies these pathways: lignocellulosic co-substrates release volatiles that influence dehydration, decarboxylation and cross-linking reactions, enhancing aromatic condensation and thereby favouring greater carbon retention, particularly in PW-rich blends. Several studies on sludge–biomass systems report similar synergistic interactions, where biomass with higher intrinsic carbon content accelerates the development of thermally stable carbonaceous structures, while feedstocks with higher ash or mineral content (such as RH) show reduced carbon retention due to catalytic effects that promote devolatilisation. These mechanistic differences are consistent with the higher carbon contents found in BS/PW mixtures and the comparatively lower values observed for BS/RH blends in this study [8,13,21,33]

Nitrogen (N) Content

N is a key component of BSs, with concentrations typically ranging between 2–8% [11,54], making it a parameter of major significance for potential agricultural applications. In the present study, the BS used for biochar production contained 6.03% N, a value that lies within this reported range and closely matches the findings of [57], who characterised BS from the same treatment facility and reported concentrations between 6.35% and 6.78%.

In the biochars produced through pyrolysis and co-pyrolysis, the total N content exhibited a clear dependence on both the pyrolysis temperature and the feedstock mixture employed. At 300 °C, N contents ranged from 6.86% in BS biochar to 3.08% in the BS/RH 1:2 mixture. At 400 °C, values varied between 5.25% in BS biochar and 2.62% in the BS/RH 1:2 mixture. Finally, at 500 °C, the lowest N concentrations were recorded, with a maximum of 4.35% in BS biochar and a minimum of 2.19% in the BS/RH 1:2 mixture (see Figure 1b–d). These results indicate that biochars derived exclusively from BSs retained the highest N contents at all temperature levels, whereas co-pyrolysis with RH, particularly at lower BS proportions (BS/RH 1:2), led to a notable reduction in N content.

Biochars obtained from BS pyrolysis exhibited the highest N concentrations, although these values decreased progressively with increasing pyrolysis temperature. This behaviour was anticipated, as sewage sludge and other animal-derived residues typically contain higher nitrogen levels than lignocellulosic biomasses, owing to the presence of proteins and nitrogen-rich compounds in their composition [31]. Furthermore, the progressive decline in nitrogen content with increasing pyrolysis temperature has been previously reported and is attributed to the thermal transformation of nitrogenous compounds, primarily amino acids, into more thermally stable structures, such as N-pyridinic and N-pyrrolic forms [11,58].

In the case of co-pyrolysis, it was observed that the addition of RH in a higher proportion (BS/RH 1:2) resulted in lower N contents across all temperature levels, which can be attributed to the low intrinsic N concentration of RH (1.05%). In contrast, co-pyrolysis with PW produced N values comparable to those obtained from BS pyrolysis, suggesting that this biomass helps to preserve relatively higher nitrogen levels in the resulting biochars. These findings confirm that the nitrogen content of biochars derived from co-pyrolysis is strongly influenced by both the type of co-substrate and the mass ratio employed, as lignocellulosic residues such as RH and PW generally possess lower N concentrations than BS [11,37,58].

When compared with the results reported by [13], the N contents of the biochars obtained in the present study were consistently higher. For instance, SS pyrolysis yielded N contents of 4.7%, 3.5%, and 2.7% at 300, 400 and 500 °C, respectively, whereas BS-derived

biochars reached 6.86%, 5.25%, and 4.35% under the same conditions. Similarly, for SS/RS (1:1) co-pyrolysis, N contents of 2.8%, 3.2%, and 2.7% were reported, compared with 4.16%, 3.58%, and 3.26% obtained in the BS/RH (1:1) mixtures. In the case of SS/SD (1:1), ref. [13] documented 1.6%, 2.6%, and 2.6%, while in this study, BS/PW (1:1) co-pyrolysis achieved 4.79%, 4.55%, and 4.05% at the same respective temperatures. This difference can be attributed to the intrinsically higher nitrogen content of BSs, previously reported by [57], which exceeds that of other organic amendments, typically characterised by N contents ranging from 1.54% to 4.07%.

The literature indicates that during pyrolysis, nitrogen is progressively incorporated into heterocyclic aromatic structures, leading to the formation of pyrogenic organic nitrogen [59–61]. Although this form of nitrogen is less bioavailable, it can still be assimilated by plants and microorganisms, thereby contributing to biomass production and the synthesis of nitrogenous compounds [61,62]. In this context, the N-enriched biochars obtained in the present study may represent promising candidates for the development of slow-release fertilisers, with the potential to minimise nitrogen losses through leaching or nitrification. Nonetheless, further research is required to assess the bioavailability and agronomic effectiveness of this nitrogen under real-field application conditions.

The decline in nitrogen content with increasing temperature reflects the progressive volatilisation of N-bearing compounds during pyrolysis, mainly through deamination reactions that release NH_3, HCN and other gaseous species. Co-pyrolysis alters these pathways: low-N substrates such as RH dilute the nitrogen-rich fraction of BS and enhance volatilisation, whereas PW, with a higher intrinsic C content, favours the partial stabilisation of nitrogen within emerging aromatic structures. Similar patterns have been reported in sludge–biomass systems, where feedstock composition determines the extent of N loss and the formation of more stable heterocyclic N forms within the char matrix [8,46].

H/C Molar Ratio

The hydrogen-to-carbon (H/C) molar ratio is a key indicator of the degree of carbonisation, structural stability, and aromaticity of biochar [11,63–65]. During pyrolysis, the thermal decomposition of hydrogen- and oxygen-containing functional groups results in their progressive removal relative to carbon, leading to a decrease in the H/C ratio [31]. This parameter is directly associated with the formation of condensed aromatic structures, which serve as a fundamental measure of the chemical recalcitrance and long-term stability of the material [10]. According to the EBC and the IBI standards, a material can be classified as biochar only if its H/C molar ratio is below 0.7 [11]. Values below this threshold denote a higher degree of carbonisation and, consequently, greater structural stability. It should also be noted that the H/C ratio is temperature-dependent, generally declining with increasing pyrolysis temperature due to enhanced aromatisation and dehydrogenation processes [11,63,65].

In this study, the H/C molar ratio of the biochars produced at 300 °C ranged from 1.18 BS to 0.98 BS/PW 1:2. At 400 °C, the maximum value was 0.82 (BS/RH 2:1), while the minimum reached 0.58 BS/RH 1:2. At 500 °C, the H/C ratios varied between 0.51 BS/RH 2:1 and 0.41 BS. Consistent with previous findings, a progressive decrease in the H/C ratio with increasing pyrolysis temperature was observed [7,11].

In relation to the EBC and IBI standards (H/C < 0.7), the results indicate that at 300 °C, none of the samples met the specified threshold. At 400 °C, five out of thirteen treatments (38.46%) complied with this criterion, whereas at 500 °C, all biochar samples exhibited H/C values below 0.7. These results suggest that biochars produced at the highest temperature attained a greater degree of aromaticity and, consequently, enhanced structural stability (see Figure 1b–d).

For BS pyrolysis, the H/C molar ratios obtained in this study were 1.18, 0.81, and 0.40 at 300, 400 and 500 °C, respectively. As expected, the increase in temperature resulted in a progressive reduction in the H/C ratio, with BS biochar at 500 °C being the only sample that satisfied the 0.7 threshold established by the EBC and the IBI. When compared with previous studies, ref. [21] reported H/C values of 1.0, 0.8, and 0.6 for biochars derived from SS at the same temperatures, results that are in close agreement with those obtained in the present work. In contrast, ref. [32] reported considerably higher H/C ratios (4.3, 4.1, and 4.3 for the same temperature range) for biochars produced from MSS. These differences can be attributed to variations in the elemental composition of the BS and sewage sludge used in each study, underscoring the influence of feedstock characteristics on the final stability of the resulting biochar.

For BS co-pyrolysis with RH or PW, it was observed that biochars derived from mixtures with a higher proportion of BSs exhibited higher H/C molar ratios. Conversely, when the lignocellulosic biomass (RH or PW) predominated, the H/C values decreased. This behaviour suggests that the presence of BS contributes to increasing the H/C ratio, consistent with the findings of [11], who reported a decreasing order of H/C ratios among different biomasses used for biochar production (manure > straw > paper waste > fish waste). Accordingly, the incorporation of lignocellulosic co-substrates appears to exert a dilution effect, lowering the H/C values of biochars produced by co-pyrolysis. However, it is important to note that neither RH nor PW induced sufficient changes to significantly alter the overall pattern observed in the co-pyrolysed biochars.

To contextualise the H/C molar ratios obtained in this study, a comparative analysis was carried out with previous research. For BS/PW (1:1) co-pyrolysis, the H/C values were 1.07, 0.73, and 0.50 at 300, 400 and 500 °C, respectively. These results exhibit a similar trend to that reported by [21] for the co-pyrolysis of SS with CS (1:1), where corresponding H/C ratios of 1.0, 0.7, and 0.7 were obtained. However, the values observed here are substantially lower than those reported by [32] for the co-pyrolysis of MSS with SD (5:5), which yielded H/C ratios of 3.6, 2.1, and 0.9. These differences further highlight the strong influence of feedstock elemental composition on the structural and chemical properties of the resulting biochars.

Similarly, the results obtained from the co-pyrolysis of BS/RH exhibited a remarkable agreement with those documented in the existing literature. For instance, ref. [2] reported an H/C ratio of 0.5 for the co-pyrolysis of MSS with RH in a 4:1 ratio at 500 °C, a value that closely aligns with the 0.51 observed in BS/RH (2:1) under identical conditions. Furthermore, ref. [32] recorded a value of 0.8 for MSS/RH in a 1:1 ratio at 400 °C, which corresponds well with the 0.79 obtained for BS/RH (1:1) at the same temperature. These consistent findings suggest that, despite variations in the biomass materials employed, the values obtained in this study are in strong alignment with those reported in prior research, thereby reinforcing the robustness and reliability of the results.

The results demonstrate that both pyrolysis and co-pyrolysis lead to a reduction in the H/C ratio as the temperature increases. Upon comparing the co-substrates, it was found that co-pyrolysis with RH results in slightly lower H/C values than co-pyrolysis with PW, suggesting that the inclusion of RH more effectively promotes the formation of stable aromatic structures. This behaviour is particularly noteworthy given that international standards, such as those outlined by the EBC and IBI, set a threshold of H/C < 0.7 for biochars to be classified as stable. Based on this criterion, the biochars produced at 500 °C, as well as a significant proportion of those produced at 400 °C, meet the established quality parameters. Among these, treatments involving RH exhibit the greatest potential for long-term agricultural and environmental applications, including soil amendments and carbon sequestration strategies.

3.2. Impact of Pyrolysis on the Surface Properties of Biochar

3.2.1. Surface Area

The surface area of biochar is a critical physicochemical parameter for its application in soils, as it defines the interface where various biological and chemical processes occur [66,67]. An increase in surface area enhances water retention, facilitates gas adsorption [31], and stimulates microbial activity [66,68–70]. In biochar production, surface area is significantly influenced by several process factors, including the type of biomass used [71], temperature, residence time during pyrolysis [36,66], and system pressure [36].

In the present study, the biochars derived from BSs exhibited surface areas of 0.82, 2.19, and 1.82 m^2/g at pyrolysis temperatures of 300 °C, 400 °C, and 500 °C, respectively (see Table 4). The highest surface area was observed for biochars produced at 400 °C, suggesting that an increase in temperature promotes surface area development. However, a slight decrease was noted at 500 °C, indicating a potential saturation point beyond which further temperature elevation may not enhance this property.

Table 4. Surface Area and Pore Size of Biochars.

Biochar		Superficial Area (m^2/g) [a]	Average Pore Size (nm) [b]	Micropore Volume (cm^3/g) [c]	Meso- and Macropore Volume (cm^3/g) [b]
BS	300 °C	0.82	3.14	3.32×10^{-5}	0.0011
	400 °C	2.19	3.13	4.25×10^{-4}	0.0026
	500 °C	1.82	5.11	5.34×10^{-4}	0.0024
BS-RH 1:1	300 °C	0.82	3.14	3.32×10^{-5}	0.0011
	400 °C	2.19	3.13	4.25×10^{-4}	0.0026
	500 °C	1.82	5.11	5.34×10^{-4}	0.0024
BS-RH 1:2	300 °C	1.80	3.14	2.14×10^{-4}	0.0024
	400 °C	2.79	3.12	5.54×10^{-4}	0.0034
	500 °C	3.68	3.13	9.31×10^{-4}	0.0045
BS-RH 2:1	300 °C	1.63	3.14	2.10×10^{-4}	0.0021
	400 °C	4.11	3.09	1.01×10^{-3}	0.0048
	500 °C	3.71	3.13	1.02×10^{-3}	0.0043
BS-PW 1:1	300 °C	1.38	3.14	1.40×10^{-4}	0.0017
	400 °C	2.18	3.50	4.19×10^{-4}	0.0029
	500 °C	3.24	3.13	7.64×10^{-4}	0.0037
BS-PW 1:2	300 °C	1.28	3.13	1.27×10^{-4}	0.0017
	400 °C	1.90	6.84	4.47×10^{-4}	0.0021
	500 °C	3.66	3.12	9.25×10^{-4}	0.0044
BS-PW 2:1	300 °C	0.93	3.13	1.91×10^{-4}	0.0020
	400 °C	1.73	5.86	3.40×10^{-4}	0.0023
	500 °C	4.62	3.10	1.17×10^{-3}	0.0052
BS-RH-PW 1:1:1	300 °C	0.58	3.54	2.09×10^{-4}	0.0015
	400 °C	2.32	3.14	5.87×10^{-4}	0.0030
	500 °C	4.86	3.10	1.15×10^{-3}	0.0047

[a] Multipoint BET, [b] BJH Method adsorption, [c] SF Method.

The biochars produced through co-pyrolysis of BSs with RH demonstrated an increase in surface area, with this effect being more pronounced in mixtures with a higher proportion of RH (Table 4). Furthermore, the enhancement in surface area was found to be temperature-dependent, as the surface areas of the BS/RH mixtures at 300 °C were lower than those obtained at 400 °C and 500 °C. Notably, the BS/RH 1:2 treatment at 400 °C yielded the highest surface area, achieving a value of 4.105 m^2/g.

Biochars produced through the co-pyrolysis of BSs with PW exhibited a behaviour similar to that observed with RH, with an increase in temperature promoting an enhancement in surface area. This effect was most pronounced at 500 °C, where the BS/PW 1:1, BS/PW 1:2, and BS/PW 2:1 treatments reached surface areas of 3661, 4617, and 3618 m^2/g, respectively. In line with the results for RH, the highest surface area was observed in the treatment with the greatest proportion of lignocellulosic biomass: in this case, PW.

In this study, it was observed that the co-pyrolysis of lignocellulosic biomass (RH and PW) resulted in biochars with a larger surface area compared to those derived exclusively from BSs (see Table 4). This effect was influenced by both the type of biomass and the temperature: RH exhibited a greater increase in surface area at 400 °C, while PW showed a more pronounced effect at 500 °C. In both cases, the proportions with the highest lignocellulosic biomass content (1:2) achieved the highest surface area values. This trend aligns with previous reports on woody biomass, where surface area increases with temperature [71], in contrast to SS, which exhibits significantly lower values [31].

In the study by [13], biochars produced from the pyrolysis of SS and its co-pyrolysis with SD and RS (1:1 ratio, 500 °C, 60 min) exhibited surface areas of 7.1, 3.9, and 6.6 m^2/g, respectively. In comparison, under similar conditions but with a shorter residence time (20 min), the surface areas obtained in this study were 1.82 m^2/g for BS, 3.66 m^2/g for BS/PW 1:1, and 3.68 m^2/g for BS/RH 1:1. While the values reported by [13] are higher, there is a notable similarity between the surface areas of SS/SD and BS/PW co-pyrolysis, suggesting a comparable effect of lignocellulosic co-substrates.

Similarly, ref. [21] reported surface areas of 15.6, 16.34, and 9.43 m^2/g for SS pyrolysis at 300, 400 and 500 °C, respectively, with a residence time of 120 min. In this study, under similar conditions but with a shorter residence time (20 min), BS biochars achieved surface areas of 0.82, 2.19, and 1.82 m^2/g at the same temperatures. Regarding co-pyrolysis, ref. [21] obtained surface areas of 14.42, 15.76, and 10.78 m^2/g for SS/CS (1:1), while in the present study, the BS/PW 1:1 co-pyrolysis showed values of 1.28, 1.90, and 3.66 m^2/g. These discrepancies highlight the influence of both the intrinsic characteristics of each biomass and the residence time, which appears to be a critical factor in the development of surface area.

A comparison with previous studies revealed that the surface area values obtained in this study were relatively low. A key distinction lies in the shorter residence time applied (20 min) compared to those used in earlier studies, such as those by [13] (60 min) and [21] (120 min). Due to the exploratory nature of this study and the high number of pyrolysed and co-pyrolysed samples, a shorter residence time was selected. Nevertheless, the results suggest that biochars with favourable characteristics for soil applications can still be identified. Future studies can evaluate the impact of variations in pyrolysis conditions, including longer residence times, to further enhance surface area.

3.2.2. Functional Groups on the Surface of Biochars and Raw Biomasses

The FTIR spectra are presented in Figure 2. Both the raw biomass (prior to heat treatment) and the biochars derived from pyrolysis and co-pyrolysis were analysed across the three temperature levels used. Overall, it was observed that an increase in temperature, coupled with the incorporation of lignocellulosic biomass (RH and PW) into the BS, resulted in significant changes to the spectral patterns.

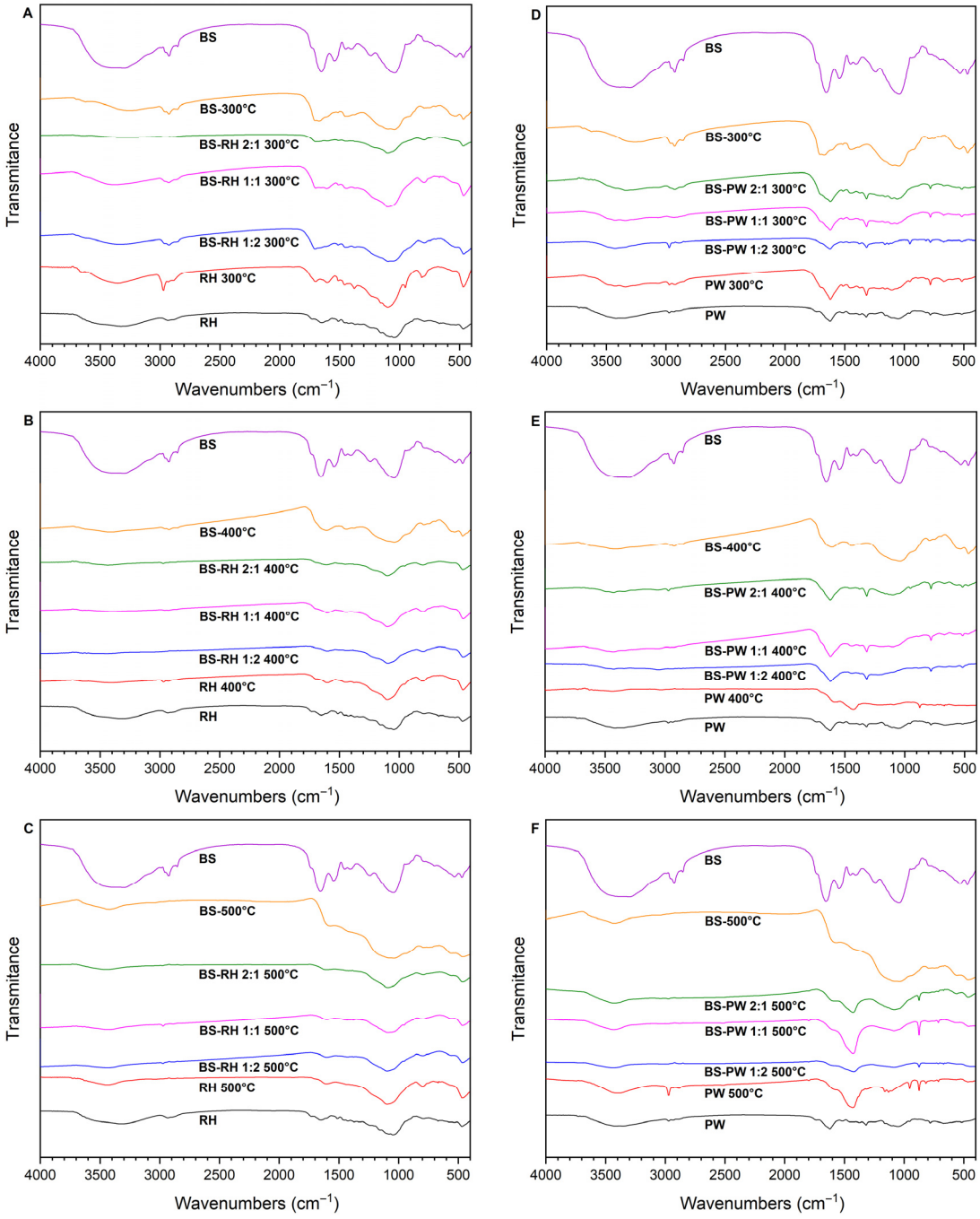

Figure 2. FTIR spectra of biochars and raw biomasses. (**A**) Differential comparison of FTIR spectra of raw biomasses and biochars derived from pyrolysis and co-pyrolysis of biochars from BS/RH mixtures at different mass ratios at 300 °C. (**B**) 400 °C. (**C**) 500 °C. (**D**) Differential comparison of FTIR spectra of raw biomasses and biochars derived from pyrolysis and co-pyrolysis of biochars from BS/PW mixtures at different mass ratios at 300 °C. (**E**) 400 °C. (**F**) 500 °C. For all sections, the spectrum of the raw biomass (BS, RH or PW, as appropriate) is shown at the ends, while the spectrum of the biomass pyrolysis and the increase in the mass proportion of the co-pyrolysis (2:1; 1:1 and 1:2) are shown inwards.

The FTIR spectra of the raw biomasses (BS, RH, and PW) exhibited both similarities and differences in their vibrational patterns. Broad bands in the range of 3400–3500 cm^{-1}, corresponding to hydroxyl groups, were identified in all three biomasses. Additionally, signals between 2850 and 2930 cm^{-1}, attributed to the C–H stretching vibrations of aliphatic compounds, fats, and lipids, were also observed [2,72,73].

The BS spectrum exhibited distinctive features associated with its higher protein content. Notably, the band at 1402 cm^{-1}, corresponding to COO^- and CH_3 vibrations, the signal at 1545 cm^{-1}, related to secondary amides, and the band at 1240 cm^{-1}, linked to C–N/N–H vibrations and phosphodiester bonds present in phospholipids and nucleic acids, were observed [57,74–78].

Both BS and RH displayed bands in the range of 875–1050 cm^{-1}, which are attributed to C–O and C–C stretching vibrations of polysaccharides and aromatic compounds, as well as signals around 450 cm^{-1}, indicative of Si–O–Si and Al–O–Si vibrations. Furthermore, both biomasses exhibited bands between 1650 and 1750 cm^{-1}, which are associated with C=O stretching vibrations of ketones, aldehydes, and carboxylic acids [32,57,79,80].

In contrast, RH and PW exhibited bands in the range of 1500–1600 cm^{-1}, corresponding to aromatic C=C and C=O vibrations, as well as a characteristic signal at 800 cm^{-1}, which is attributed to aromatic compounds [18,32,81,82]. Additionally, PW displayed distinctive bands at 1317 and 1053 cm^{-1}, associated with alkyl ether structures, which were absent in both BS and RH [47].

In the FTIR spectra of biochars obtained from BS/RH pyrolysis (see Figure 2A–C), various signals were observed, reflecting structural modifications compared to the raw biomasses. The broad band in the range of 3400–3500 cm^{-1}, attributed to hydroxyl groups, remained present but showed lower intensity as the proportion of RH in the mixture increased. Additionally, signals in the 2850–2930 cm^{-1} range, corresponding to vibrations of aliphatic groups (alkane methylene), were identified in all mass ratios (BS/RH 1:2, 1:1, and 2:1) [2,72,73].

The aromatic regions were also clearly evident. In the BS/RH 1:2 and 2:1 mixtures, bands in the 1700–1600 cm^{-1} range were detected, indicating symmetric C=C stretches in aromatic fractions. Meanwhile, in the BS/RH 1:1 mixture, vibrations in the 1600–1500 cm^{-1} range suggested the presence of C–C aromatic structures. Furthermore, the signal at 1415 cm^{-1}, observed in both BS/RH 1:2 and 1:1 mixtures, confirmed the presence of aromatic rings and/or inorganic carbonates [45,83,84].

All evaluated proportions displayed bands in the 1080–1050 cm^{-1} range, corresponding to asymmetric C–O–C and C–C–O stretching vibrations, characteristic of ether linkages. Similarly, the signal at 795 cm^{-1} was observed in all combinations, indicating the presence of aromatic and heteroaromatic compounds. Additionally, bands around 450 cm^{-1}, associated with metal–halogen bond vibrations (Si–O–Si and Al–O–Si), were detected in all BS/RH biochars [13,32].

Overall, these findings suggest that co-pyrolysis with RH promotes the formation and retention of stable aromatic structures and inorganic groups, which enhances resistance to degradation and underscores the significant potential of these biochars for soil remediation and conditioning applications.

In the FTIR spectra of biochars obtained from BS/PW co-pyrolysis (see Figure 2D–F), several signals indicative of structural modifications induced by temperature and mass ratio were identified. A broad band in the 3400–3500 cm^{-1} range, attributed to hydroxyl groups, was observed in all samples, although its intensity progressively decreased with increasing temperature and PW content in the mixture [2,73]. Similarly, vibrations characteristic of aliphatic groups (alkane methylene) in the 2850–2930 cm^{-1} range were detected in all mass ratios (BS/PW 1:2, 1:1, and 2:1) [72,73].

A prominent signal at 1620 cm^{-1}, present in all three ratios, was attributed to C=O, C=C, and –CONH vibrations, suggesting the presence of aromatic rings and amide bonds, likely originating from condensed protein and aromatic fractions [2,73]. Additionally, a band at 1438 cm^{-1} was recorded in the BS/PW 1:1 and 2:1 mixtures, associated with vibrations of CHx groups in aliphatic chains and cyclic compounds [73,85].

Furthermore, signals in the 1300–1200 cm^{-1} and 1150–1050 cm^{-1} regions, observed in all proportions, were attributed to C–O–C and C–C–O stretching vibrations, characteristic of mixtures of alkyl and aromatic ethers [86].

Overall, the results indicate that PW-assisted co-pyrolysis promoted the retention of oxygenated and nitrogenated functional groups (hydroxyls, carbonyls, and amides), alongside the formation of stable aliphatic and aromatic structures. This suggests that BS/PW biochars possess a more diverse functional character, which could enhance their surface reactivity and make them more suitable for applications in adsorption processes and interactions with organic compounds in soils.

FTIR analysis revealed notable differences between raw biomass and biochars obtained through the co-pyrolysis of BS/RH and BS/PW. In general, raw biomass exhibited a broader diversity of functional groups, particularly in BS, where signals associated with proteins, lipids, and phosphorus compounds were detected. Following co-pyrolysis, a progressive reduction in the bands corresponding to hydroxyl and aliphatic groups was observed, likely due to thermal decomposition. In both BS/RH and BS/PW mixtures, there was an increase in aromatic signals (C=C, C=O) and ether structures (C–O–C, C–C–O), indicating a transformation towards more stable and condensed compounds.

From the perspective of soil applications, this transformation suggests that biochars generated by co-pyrolysis exhibit greater chemical stability and resistance to microbial degradation, favouring their long-term persistence as soil amendments. However, the reduction in oxygenated functional groups, such as hydroxyls and carboxyls, may limit their capacity for nutrient and water retention. This implies that the effectiveness of co-pyrolysis biochars will depend on the specific soil type and the agricultural management practices employed. Overall, the results indicate that co-pyrolysis biochars function more as structural materials and carbon stabilisers in soil, while raw biomasses provide a higher content of labile functional groups, which are more pertinent to immediate soil fertility.

3.2.3. Morphological and Microscopic Characteristics of BSs and Biochars

SEM analysis enabled the observation of morphological changes induced by the pyrolysis of BSs at varying temperatures (Figure 3). In its raw state, BS exhibited no defined pores, with irregularly shaped particles and a rough surface, consistent with previous reports [13,33,87]. Following pyrolysis, microstructural modifications were evident, including the formation of pores and smoother regions (Figure 3). These changes correlate with the results obtained via the BET method (Table 4), which showed an increase in surface area (0.82, 2.19, and 1.82 m^2/g) and micropore volume (3.32×10^{-5}, 4.25×10^{-5}, and 5.34×10^{-5} cm^3/g) at 300, 400 and 500 °C, respectively.

In general, co-pyrolysis resulted in an increase in surface area and micropore volume with rising temperature (see Table 4). The addition of RH and PW did not cause significant variations in these parameters; however, the 1:2 (RH/PW) ratio yielded the highest values for both surface area and micropore volume. SEM micrographs qualitatively support these trends, showing increased surface roughness, cavities and heterogeneous pore development associated with the thermal decomposition of lignin, cellulose and hemicellulose in lignocellulosic biomass during pyrolysis, rather than definitive evidence of regular or ordered pore structures [88].

In the case of BS/RH co-pyrolysis, micrographs (Figure 4) revealed network-like structures with skeletal morphology, accompanied by macropores and micropores uniformly distributed across the surface of the biochar [88]. At 500 °C, pores arranged in channel-like formations were observed [87] (see Figure 4). Biochars with a higher proportion of RH exhibited surfaces covered with small granules, a feature attributed to the release of gaseous products during pyrolysis [46]. These morphological changes were reflected in the results

obtained via the BET method, where the BS/RH ratio of 1:2 exhibited the highest values for surface area (1.63, 4.11, and 3.71 m^2/g) and micropore volume (2.10×10^{-4}, 1.01×10^{-3}, and 1.02×10^{-3} cm^3/g) at 300 °C, 400 °C, and 500 °C, respectively (see Table 4).

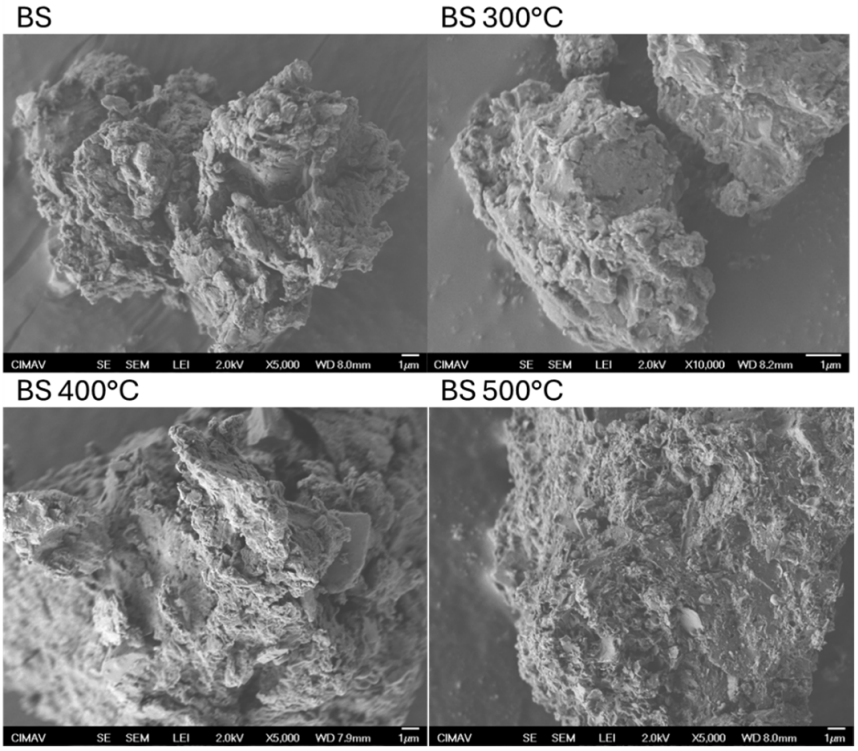

Figure 3. Micrographs of BSs and Biochars derived from BS pyrolysis at 300 °C, 400 °C and 500 °C.

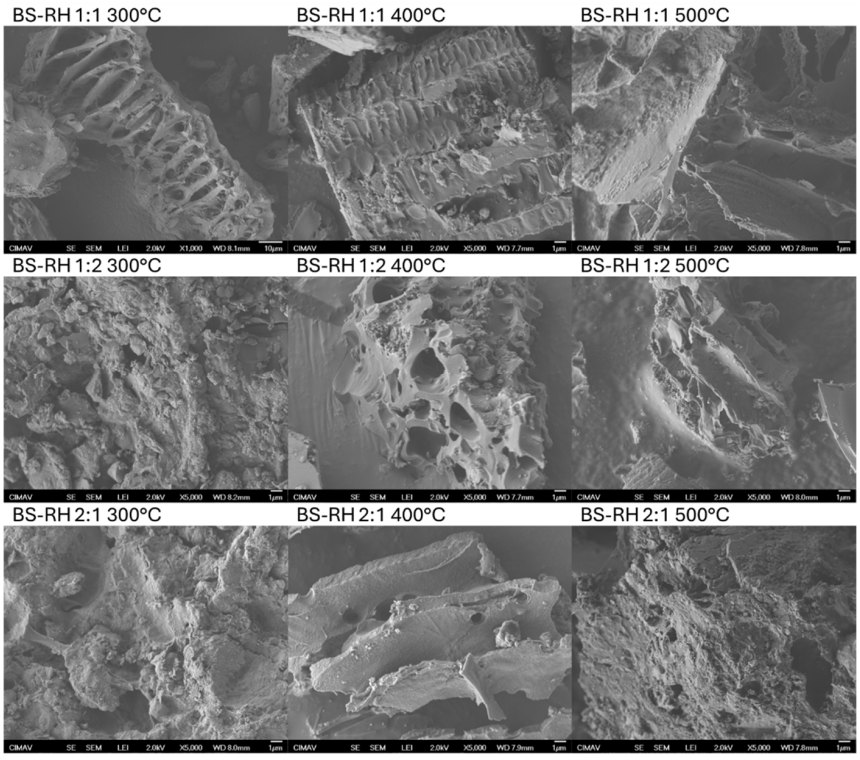

Figure 4. Micrographs of Biochars obtained from BS/RH Co-pyrolysis in their different mass proportions at the three temperature levels 300 °C, 400 °C and 500 °C.

In BS/PW co-pyrolysis, micrographs revealed cylindrical and honeycomb-shaped structures, consistent with the findings reported by [46]. At 300 °C, the biochars exhibited smoother surfaces, whereas at 400 °C and 500 °C, rougher surfaces with increased porosity were observed (Figure 5). In general, variations in mass proportions did not lead to significant morphological differences; however, the BS/PW 1:2 treatment at 500 °C stood out, achieving the largest surface area (4.65 m^2/g) and a microporous volume of 1.17×10^{-3} cm^3/g—values closely matching those obtained in co-pyrolysis with RH (see Table 4).

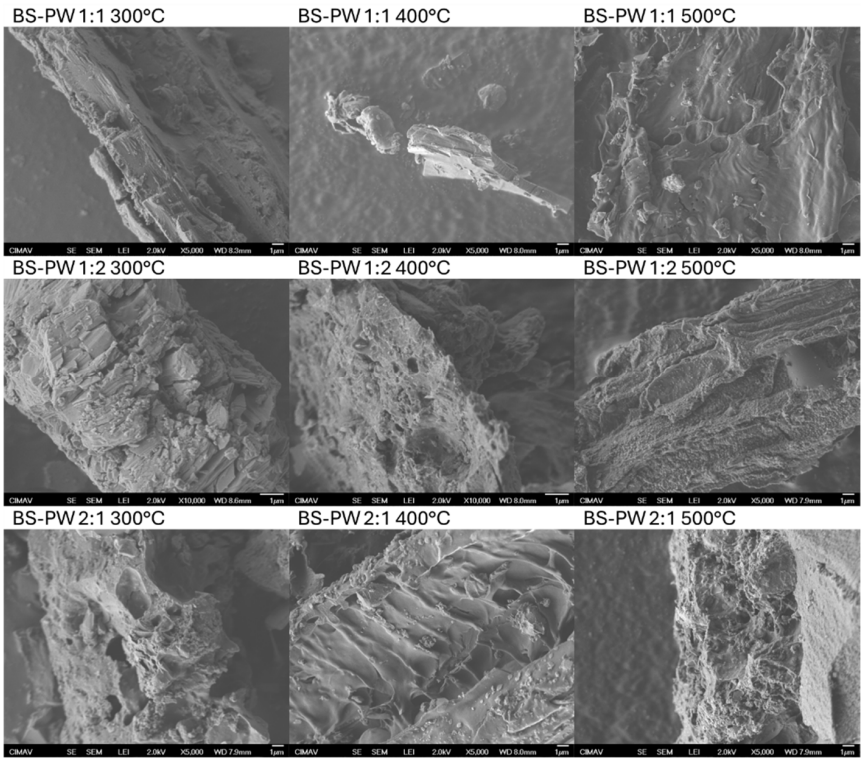

Figure 5. Micrographs of Biochars obtained from BS/PW Co-pyrolysis in their different mass proportions at the three temperature levels 300 °C, 400 °C and 500 °C.

SEM analysis revealed that the development of porosity and internal surface area is a critical characteristic of biochars for their potential agronomic applications, as these properties directly influence interactions with nutrients, contaminants, water retention, and ion exchange capacity [45,86,89]. The porosity of biochar is influenced by factors such as temperature, residence time, and reactor type [48]. In this study, it was observed that co-pyrolysis enhanced both surface area and pore volume, particularly in the 1:2 mass ratios with RH and PW. High-porosity biochars provide substantial agronomic benefits, acting as adsorbents for HMs by attracting ions and reducing contaminants [46,90]. Moreover, these biochars contribute to pH neutralisation and increase cation exchange capacity, thus improving soil fertility [47].

The results of the EDS analysis are presented in Figures 6–8. In raw BSs, carbon (C) and oxygen (O) were predominantly identified, along with smaller amounts of silicon (Si), phosphorus (P), aluminium (Al), magnesium (Mg), sulphur (S), calcium (Ca), potassium (K), and iron (Fe). Following pyrolysis at 300, 400 and 500 °C, the elemental profile remained largely unchanged, with the exception of a marked increase in the Si signal as the temperature rose (see Figure 6).

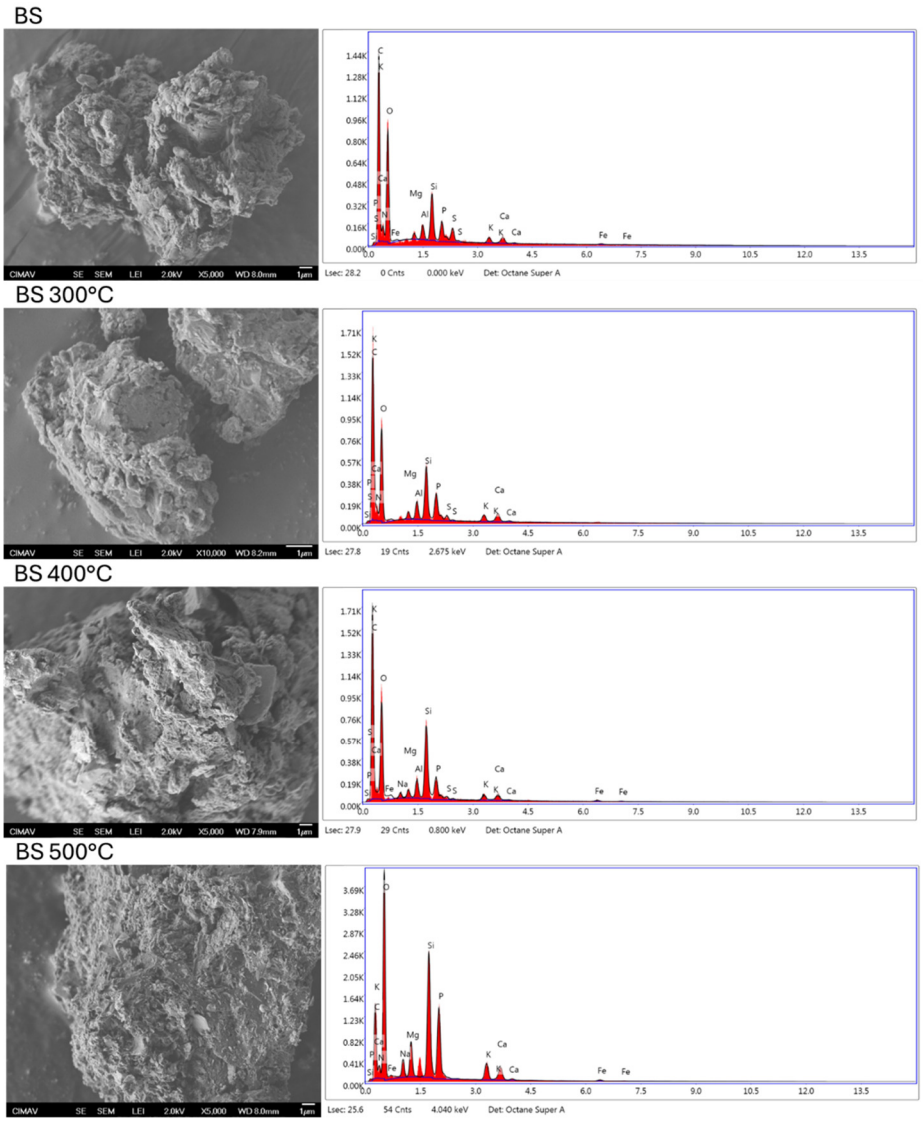

Figure 6. Micrographs and EDS spectra of crude BSs and biochars derived from BS pyrolysis at 300 °C, 400 °C and 500 °C.

In BS/RH co-pyrolysis, variations were observed in the elemental profile. For the 1:1 mass ratio, the highest concentrations of elements were recorded at 300 °C. However, as the temperature increased, the concentration of most elements decreased, except for Si, which exhibited a progressive increase (see Figure 7a). In the BS/RH 1:2 combination (see Figure 7b), the elemental profile remained generally stable, although fluctuations were observed with temperature, without a clear pattern, and with Si again showing a marked increase. In the BS/RH 2:1 ratio, elemental concentrations generally decreased with increasing temperature (see Figure 7c), although Si concentrations increased at 300 °C and 400 °C. At 500 °C, however, the concentrations of Ca and P increased.

In BS/PW co-pyrolysis, the spectra obtained displayed patterns that varied with both mass ratio and temperature. For the 1:1 combination (see Figure 8a), the profile closely resembled that of other biochars, showing fluctuations in element concentrations and a progressive increase in Si. In the 1:2 ratio (see Figure 8b), a general decrease in elemental content was observed; as the temperature increased, some elements were no longer detected, while others, such as Ca at 400 °C and P at 500 °C, showed an increase in intensity. In the 2:1 combination (see Figure 8c), there was an initial increase in the number of detected elements, followed by a decrease in their intensity as the temperature increased, with the progressive rise in Si being particularly notable.

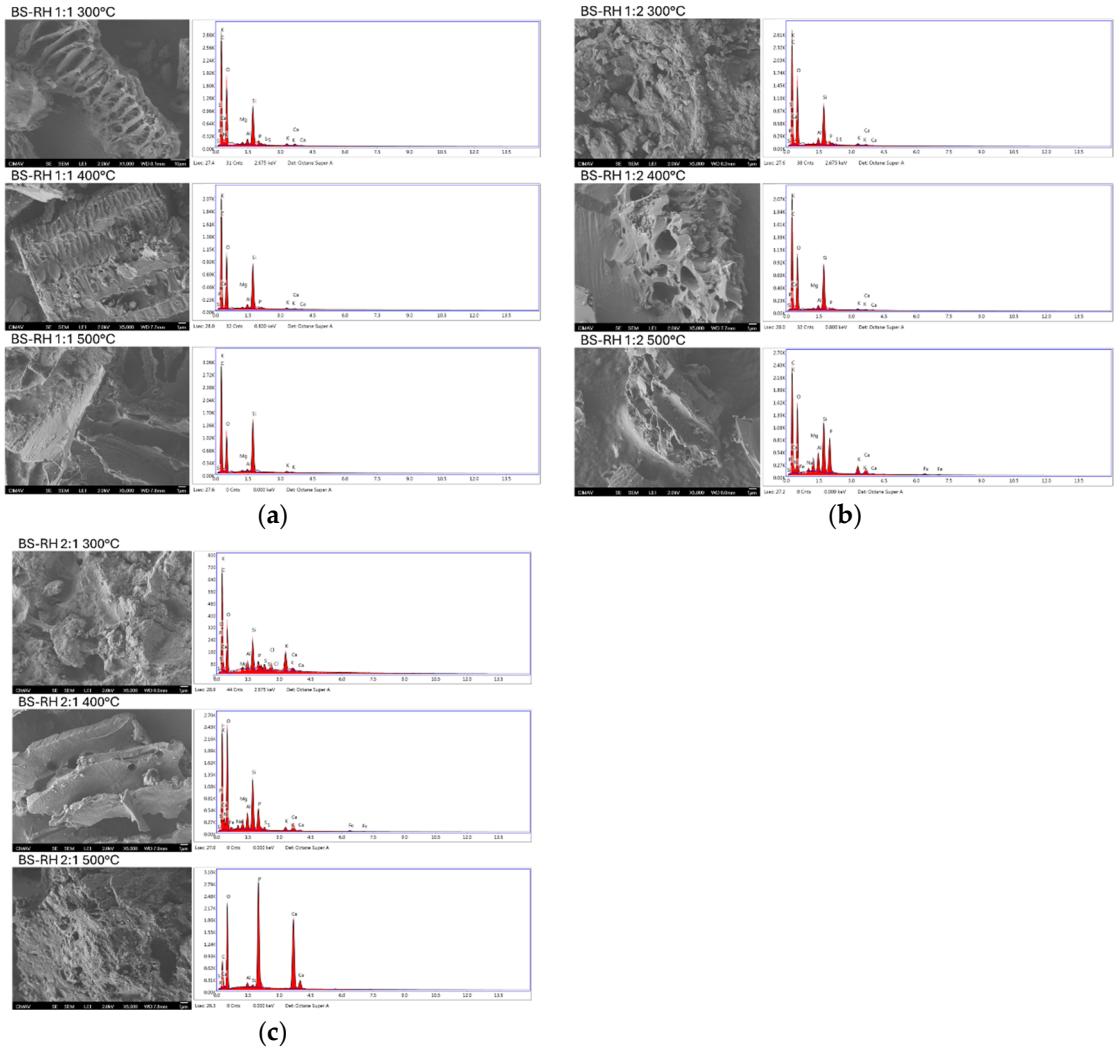

Figure 7. SEM micrographs and EDS spectra of biochars derived from BS/RH co-pyrolysis. (**a**) Biochars derived from BS/RH 1:1 co-pyrolysis at 300 °C, 400 °C and 500 °C. (**b**) Biochars derived from BS/RH 1:2 co-pyrolysis at 300 °C, 400 °C and 500 °C. (**c**) Biochars derived from BS/RH 2:1 co-pyrolysis at 300 °C, 400 °C and 500 °C.

In general, the elemental profiles on the surfaces of biochars obtained from the pyrolysis of BSs were higher than those recorded for biochars produced via co-pyrolysis with RH and/or PW. As the mass ratio of lignocellulosic biomass increased (BS/RH 1:2 and BS/PW 1:2), the elemental profile on the surface of the biochars tended to decrease. In contrast, when the mass ratio of BS was increased (BS/RH 2:1 and BS/PW 2:1), an increase in the number of detected elements was observed, which can be attributed to a dilution effect caused by the addition of lignocellulosic biomass. It is noteworthy that no HMs were detected on the surface of the biochars [23] (see Figures 7 and 8a–c). Si was identified in all treatments, with its concentration increasing with temperature. This trend was particularly pronounced in biochars derived from BS/RH pyrolysis. These findings align with those of [23], who attributed the increase in Si concentration to the elevated silica content in biochars.

From an agronomic standpoint, the detected elemental profile holds significant relevance, as the absence of HMs suggests that the biochars are environmentally safe. The presence of elements such as Ca, K, Mg, and P, albeit in varying concentrations, may promote nutrient availability in the soil. Moreover, the increased silica concentration could potentially enhance crop resilience to both biotic and abiotic stresses. Collectively, the

results from EDS highlight the potential of these biochars as agricultural amendments, not only for improving soil fertility but also for providing chemical stability and ensuring environmental safety.

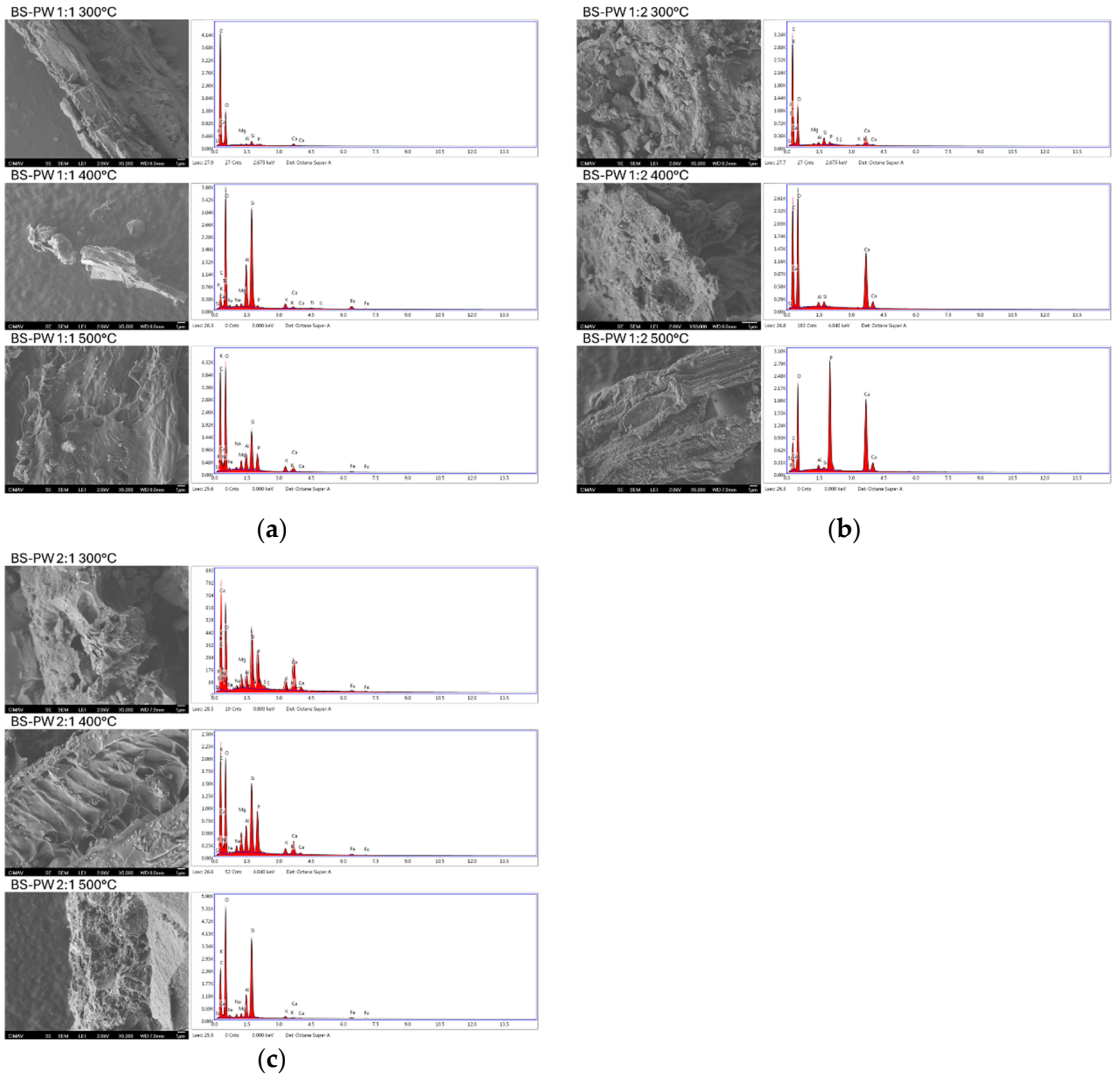

Figure 8. SEM micrographs and EDS spectra of Biochars derived from BS/PW co-pyrolysis. (**a**) Biochars derived from BS/PW 1:1 co-pyrolysis at 300 °C, 400 °C and 500 °C. (**b**) Biochars derived from BS/PW 1:2 co-pyrolysis at 300 °C, 400 °C and 500 °C. (**c**) Biochars derived from BS/PW 2:1 co-pyrolysis at 300 °C, 400 °C and 500 °C.

3.3. Metal (Oids) in Biosolids and Biochars

BSs tend to accumulate HMs, which exhibit low biodegradability due to the physico-chemical processes involved in wastewater treatment [3,51]. The primary sources of these metals include industrial wastewater discharges, food consumption, pharmaceuticals, cosmetics, and surface runoff, which contributes smaller quantities to wastewater streams [1]. The presence of HMs in BSs poses a potential risk, as these metals can enter the food chain through plant uptake. Therefore, determining their concentrations in BSs and BS-derived products is crucial for assessing their suitability for agricultural applications [3]. In this study, the total concentrations of Cd, Cr, Cu, Ni, Pb, Fe, and Zn were quantified in raw BSs and in biochars obtained through both pyrolysis and co-pyrolysis of BSs with RH and PW.

SS is the solid fraction separated during wastewater treatment, while BSs are sludges that have been treated to comply with local regulations concerning HMs and pathogens, making them suitable for agricultural use [3]. This study utilised raw BSs

(see Materials and Methods), with the characterisation focusing on the determination of HM concentrations for comparison with the permissible limits established by Mexican regulation NOM-004-SEMARNAT-2002, as well as USA (United States of America) and EU (European Union) standards. The results (Table 5) indicated that all concentrations were below the permissible limits; Cd was not detected using the applied methodology, and although Fe is not specified in the regulations, it was included in the analysis due to its importance in agricultural applications. The order of abundance of HMs in BSs was as follows: Fe > Zn > Cu > Cr = Ni > Pb.

Table 5. HMs present in the BSs used in this study and their comparison with previous studies and international parameters.

HM (mg kg^{-1})	HM This Study	Medina et al. [57]	MPL of Contaminants in Biosolids		
			Mexico	USA	EU
As	N/R	1.81	75	41	N/R
Cd	N/D	7.41	85	39	20–40
Cr	30	28.46	3000	N/R	N/R
Cu	80	107.28	4300	1500	1000–1750
Pb	10	38.19	420	300	750–1200
Hg	N/D	1.03	840	17	16–25
Ni	30	30.19	57	420	300–400
Zn	490	707.95	7500	2800	2500–4000
Fe	4960	17,340	N/R	N/R	N/R

MPL Maximum permissible limit, USA, EU, N/R Not regulated, N/D Not detected.

When comparing the results of this study with those reported by [57] from the same treatment plant in Celaya, Guanajuato, who recorded average concentrations of 17.34 g/kg (Fe), 707.95 mg/kg (Zn), 107.28 mg/kg (Cu), 28.46 mg/kg (Cr), 30.19 mg/kg (Ni), and 38.19 mg/kg (Pb), the values obtained in this study were lower: 4.96 g/kg (Fe), 490 mg/kg (Zn), 80 mg/kg (Cu), 30 mg/kg (Cr), 30 mg/kg (Ni), and 10 mg/kg (Pb). These differences can be attributed to the fact that [57] analysed half-yearly averages, while the present study analysed a single sample collected in November, reflecting the temporal variability in the composition of BSs.

A key aspect of BS characterisation is the comparison of their HM content with other by-products of wastewater treatment, such as SS. In this context, ref. [73] reported concentrations of 1729 mg/kg (Zn), 111.83 mg/kg (Cu), 94.25 mg/kg (Cr), 30.92 mg/kg (Ni), and 50.08 mg/kg (Pb) in SS. In contrast, the values obtained in the present study were lower for all metals except nickel (Ni), whose concentration was similar in both cases. This finding confirms the reduction in metal content in BSs compared to SS.

For biochars obtained through the pyrolysis of BSs, a progressive increase in HM concentration was observed as the temperature rose. This enrichment can be attributed to the greater thermal stability of HMs [13], in contrast to organic compounds, which decompose and volatilise during the pyrolysis process [5]. Although a fraction of the HMs may migrate to the liquid and gas phases, the majority remain retained in the carbonaceous matrix [5,91], resulting in a higher relative concentration as pyrolysis progresses.

In this study, the HM contents in BS-derived biochars were as follows: at 300 °C, 777 mg/kg (Zn), 130 mg/kg (Cu), 40 mg/kg (Cr), 40 mg/kg (Ni), and 30 mg/kg (Pb); at 400 °C, 920 mg/kg (Zn), 150 mg/kg (Cu), 50 mg/kg (Cr), 50 mg/kg (Ni), and 40 mg/kg (Pb); and at 500 °C, 1080 mg/kg (Zn), 160 mg/kg (Cu), 60 mg/kg (Cr), 40 mg/kg (Ni), and 50 mg/kg (Pb). The concentration pattern remained consistent, similar to that observed in raw BS, following the order: Fe > Zn > Cu > Cr = Ni > Pb.

These results align with those reported by [7], who indicated that the sequence of HM abundance in biochars derived from municipal sewage sludge is typically Zn > Cu > Cr > Pb > Ni > Cd. In this study, Zn was the predominant element, a trend consistent with previous research, and is often attributed to the widespread use of galvanized steel pipes in sewage systems [21,73,92].

To analyse the effect of co-pyrolysis of BSs with RH and PW on HM content, heat maps were generated to visualise the variations in their concentrations (see Figure 9). In general, biochars derived from BS pyrolysis exhibited higher HM concentrations compared to those obtained through co-pyrolysis, with the exception of Cr and Ni (see Figure 9a,c), whose concentrations increased with the addition of RH. The observed decrease in Zn, Pb, and Cu concentrations in co-pyrolysis can be attributed to the 'dilution effect,' a phenomenon extensively documented in the literature [13,18,93]. This effect is linked to the nature of lignocellulosic biomass (from agricultural and forestry sources), which is primarily composed of lignin, cellulose, and hemicellulose, in contrast to BSs, which are richer in proteins, fats, cellulose, and carbohydrates [6,94]. Consequently, lignocellulosic biomasses provide higher amounts of carbon and contain much lower concentrations of HMs compared to BSs [1,6,9].

A notable exception was observed in the case of Cr in biochars obtained from BS/RH co-pyrolysis. This behaviour was previously reported by [2], who found that co-pyrolysis of SS with RH increased the concentration of Cr, attributed to the high content of this metal in the original biomass. Similarly, ref. [18] reported that co-pyrolysis of reed (*Phragmites australis*) with SS maintained high Cr levels, reflecting the composition of both precursor materials. In the present study, a similar effect was observed in the BS/RH mixture for both Cr and Ni.

In contrast, the increase in these metals was not observed in BS/PW co-pyrolysis, suggesting that PW contains minimal amounts of Cr or Ni, making it a more suitable biomass for biochar production with lower heavy metal accumulation. These findings underscore the importance of biomass selection in co-pyrolysis, as it influences not only the physicochemical properties of the biochar but also its compliance with the quality and safety standards required for agricultural applications. Consequently, it is crucial to compare the obtained parameters with current international regulations.

Biochar certification and commercial use are currently regulated by two main international initiatives: the EBC and the IBI [11]. Both initiatives have established comprehensive guidelines for physicochemical parameters, with a particular focus on HM limits for biochar intended for soil application. In this study, the HM contents in biochar obtained from both BS pyrolysis and co-pyrolysis with RH and PW were compared with the maximum allowable concentrations set by these certifications (see Figure 10). This comparison is essential, as it facilitates the assessment not only of the suitability of the produced biochars as soil amendments but also of the impact of co-pyrolytic biomass on compliance with these international standards.

When comparing the biochars with the reference values established by the IBI, notable differences were observed based on both the pyrolysis temperature and the biomass used in co-pyrolysis. At 300 °C (see Figure 10b), Cr, Cu, Pb, and Ni remained below the limits in all biochar samples, while Zn exceeded the reference value in most cases, with the exception of the BS/RH/PW 1:1:1, BS/PW 1:2, and BS/RH 1:2 treatments. At 400 °C (see Figure 10d), Cr and Pb remained consistently below the limit across all treatments, with Cu exceeding the limit only in BS biochar, and Ni exceeding the limit only in BS and BS/RH 1:2. Zn was again the most restrictive metal, with only the BS/RH/PW 1:1:1 treatment remaining below the established value. Finally, at 500 °C (see Figure 10e), Cr, Pb, and Ni remained within acceptable concentrations in all biochars, while Cu exceeded the limit only in BS

and BS/RH 2:1 biochars. At this temperature, Zn continued to be the critical metal, with only the BS/RH 1:2 treatment staying below the established limit.

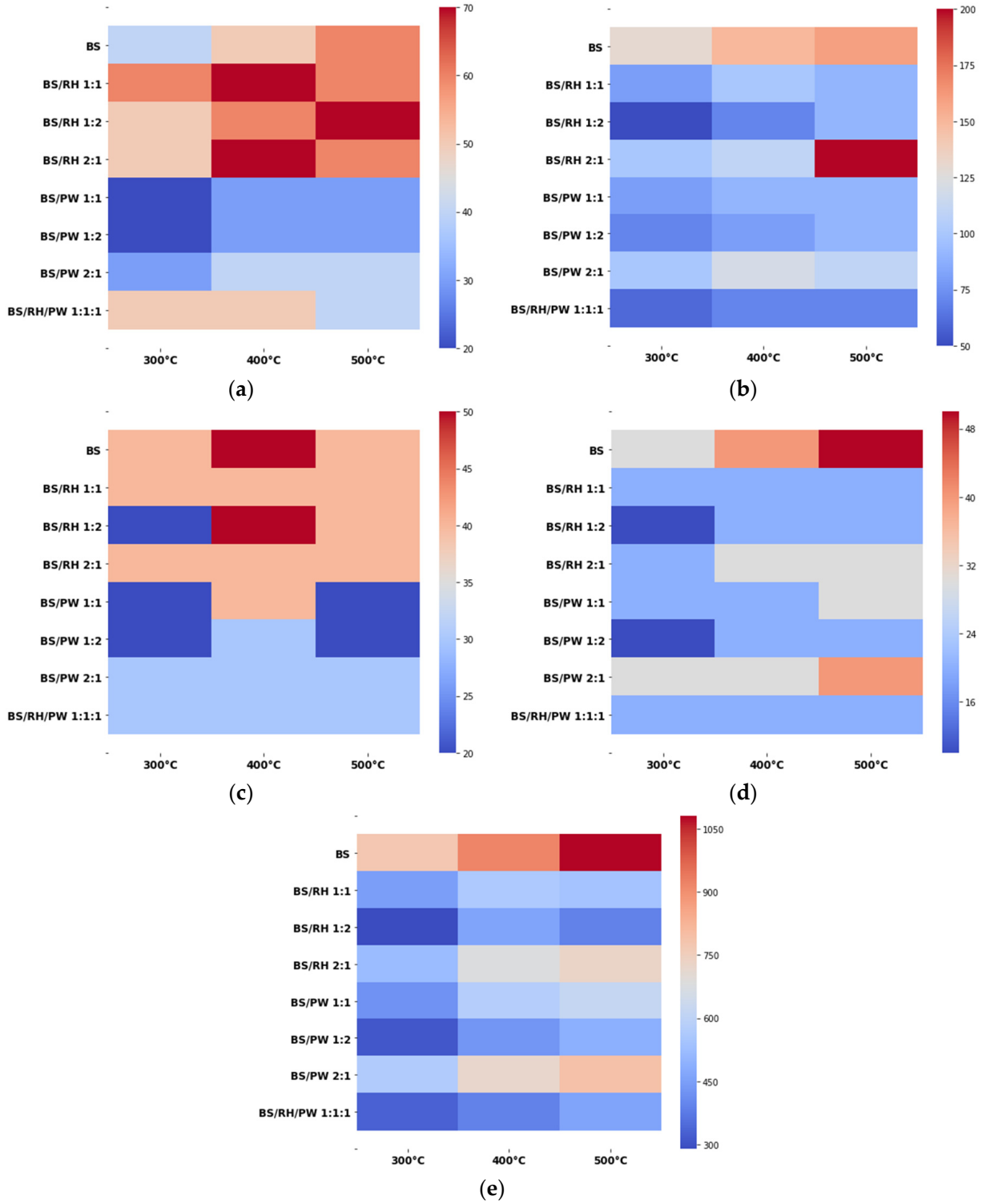

Figure 9. Heat graphs for comparing heavy metal content fluctuations in BS pyrolysis and co-pyrolysis with RH and PW. (**a**) Cr, (**b**) Cu, (**c**) Ni, (**d**) Pb and (**e**) Zn.

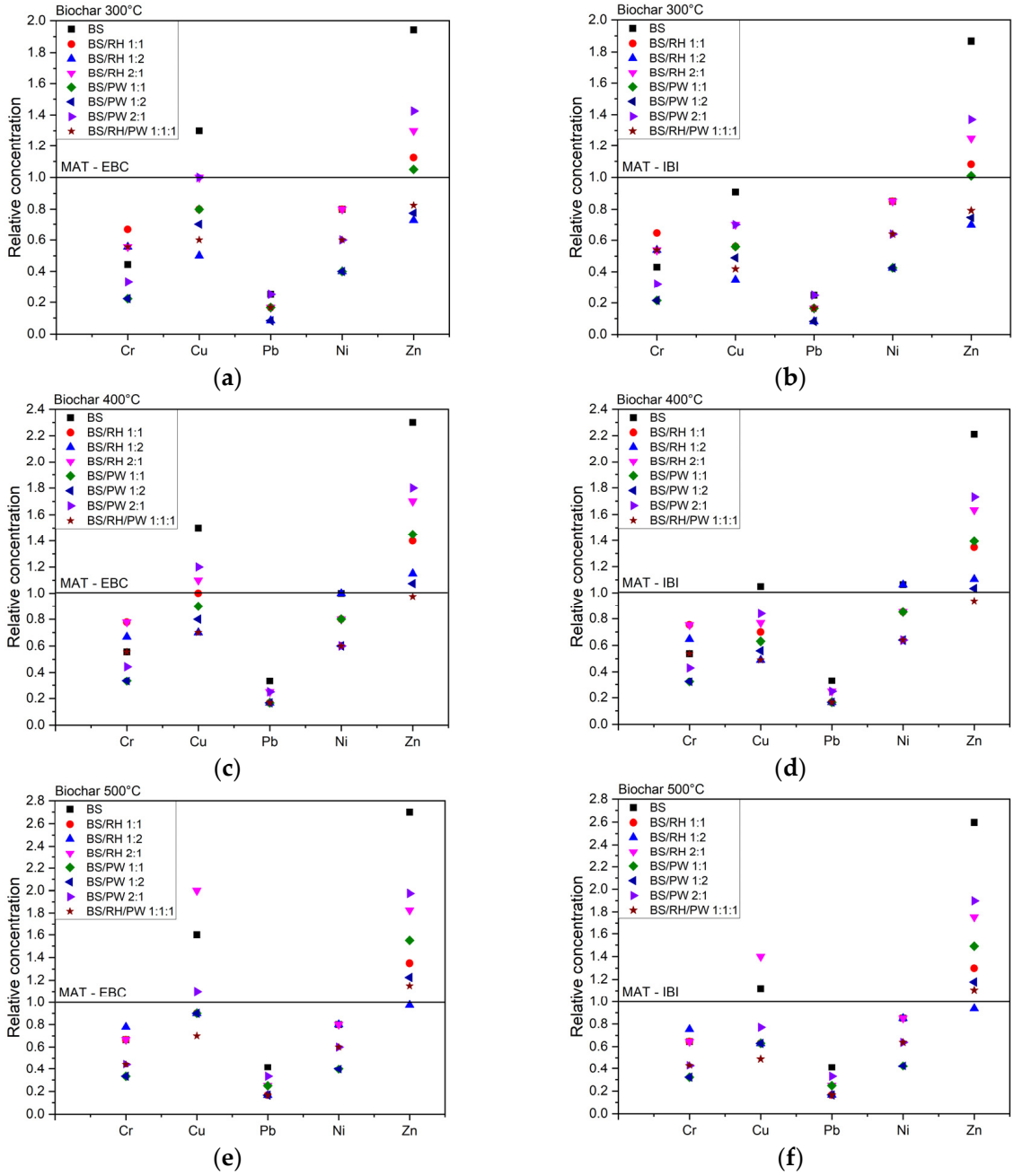

Figure 10. HM content in biochars obtained from pyrolysis of BSs and in co-pyrolysis with RH and PW according to the limits declared by the IBI and EBC. (**a**) Biochars obtained at 300 °C compared to the values declared by the EBC. (**b**) Biochars obtained at 300 °C compared to the values declared by the IBI. (**c**) Biochars obtained at 400 °C compared to the values declared by the EBC. (**d**) Biochars obtained at 400 °C compared to the values declared by the IBI. (**e**) Biochars obtained at 500 °C compared to the values declared by the EBC. (**f**) Biochars obtained at 500 °C compared to the values declared by the IBI.

When comparing the results with the reference values established by the EBC, the biochars obtained at 300 °C (see Figure 10a) showed that Cr, Pb, and Ni concentrations were below the limit in all cases. Cu remained within the permitted value, except in the biochar derived exclusively from BSs. For Zn, only the BS/RH 1:2, BS/PW 1:2, and BS/RH/PW 1:1:1 combinations met the standard, while the other treatments exceeded the established limit. At 400 °C (see Figure 10c), Cr, Pb, and Ni concentrations remained within acceptable levels in all treatments, while Cu exceeded the limit in BS, BS/PW 2:1, and BS/RH 2:1.

Zn continued to be the most restrictive metal, with only the BS/RH/PW 1:1:1 treatment remaining below the limit. Finally, at 500 °C (see Figure 10d), Cr, Pb, and Ni remained below the reference values, while Cu exceeded the limit in BS, BS/RH 2:1, and BS/PW 2:1. As observed at the other temperatures, Zn was the most problematic metal, with only the BS/RH 1:2 treatment complying with the EBC-established value.

In comparing the reference values established by the IBI and the EBC, Cu and, particularly, Zn most frequently exceeded the established limits. This underscores the need for further investigation into these metals to ensure that biochar application does not pose a risk to soil or groundwater contamination. In addition to regulatory compliance, understanding the mechanisms that govern HM behaviour in biochar is essential for assessing its agricultural and environmental suitability. Overall, all biochars met the maximum allowable concentrations for Cr, Pb and Ni, whereas Cu and particularly Zn exceeded the thresholds in several BS-and BS/RH-derived materials, making Zn the most restrictive element across treatments. Regarding structural stability, only the biochars produced at 400 and 500 °C met the H/C requirements of IBI (<0.7) and EBC (<0.6), indicating sufficient aromatic condensation. However, the environmental relevance of HMs is determined not only by their total concentrations but also by their mobility and leaching potential. Previous studies have shown that increasing pyrolysis temperature promotes the formation of metal–silicate, metal–phosphate and metal–oxide phases, as well as the encapsulation of metals within carbonaceous structures, thereby reducing their solubility and bioavailability [8,13,21,33]. Co-pyrolysis can further enhance these immobilisation pathways by diluting metal-rich BSs with lignocellulosic biomass and facilitating the incorporation of metals into more recalcitrant mineral matrices. Thus, although Cu and Zn exceed regulatory thresholds in some treatments, the reduced mobility associated with these stabilisation processes suggests that their environmental risk may be substantially lower than implied by total concentrations alone. Nevertheless, targeted leaching assays are required to confirm the extent of metal immobilisation and establish the safe agricultural use of the produced biochars.

However, several studies have shown that metals such as Cu, Cr, Zn, Pb, Mn, and Ni tend to transform into more stable forms during pyrolysis, reducing both their immediate phytotoxicity and bioavailability [53]. Therefore, future research should focus on evaluating these transformations and their impact on the environmental safety of biochar. It is important to note, however, that chemical characterisation alone is insufficient for assessing the viability of biochar in agricultural applications. Consequently, examining the direct effects of biochars on the growth and development of crops of interest, such as maize, is essential, as maize serves as a relevant model due to its agronomic and food significance.

3.4. Effect of Biochar on Corn Plant Growth

Impact of Biochar Addition on Seed Germination, Plant Weight, and Biomass Production

Seedling germination and growth tests are among the most straightforward and effective methods for assessing the quality of biochar and its potential impact on plant yield in the short term [50,95–97]. Consistent with this, the IBI includes germination tests in its assessment guidelines as an initial criterion for validating the agricultural application of biochar [10]. In this context, the present study conducted an experiment using *Zea mays*, a crop of significant food and economic importance in Mexico, to evaluate the effects of biochar derived from the pyrolysis of BSs and its co-pyrolysis with RH and PW. The physiological parameters assessed included the RSGR, RRG, GI, as well as fresh weight (FW) and dry weight (DW). The results are presented in Table 6 and Figure 11.

Table 6. Germination results for the various treatments using biochars derived from BS pyrolysis and co-pyrolysis with RH and PW.

Treatment	RSGR %	RRG %	GI %
BS-300 °C	83.33	284.31	29.31
BS-400 °C	100.00	144.12	69.39
BS-500 °C	83.33	144.12	57.82
BS-RH 1:1-300 °C	100.00	250.00	40.00
BS-RH 1:1-400 °C	100.00	274.51	36.43
BS-RH 1:1-500 °C	83.33	251.96	33.07
BS-RH 1:2-300 °C	83.33	136.27	61.15
BS-RH 1:2-400 °C	100.00	240.20	41.63
BS-RH 1:2-500 °C	100.00	404.90	24.70
BS-RH 2:1-300 °C	125.00	145.10	86.15
BS-RH 2:1-400 °C	83.33	301.96	27.60
BS-RH 2:1-500 °C	100.00	308.82	32.38
BS-PW 1:1-300 °C	100.00	207.84	48.11
BS-PW 1:1-400 °C	125.00	146.08	85.57
BS-PW 1:1-500 °C	166.67	204.90	81.34
BS-PW 1:2-300 °C	125.00	217.65	57.43
BS-PW 1:2-400 °C	125.00	72.55	172.30
BS-PW 1:2-500 °C	125.00	111.76	111.84
BS-PW 2:1-300 °C	100.00	293.14	34.11
BS-PW 2:1-400 °C	125.00	131.37	95.15
BS-PW 2:1-500 °C	166.67	387.25	43.04
BS-RH-PW 1:1:1-300 °C	83.33	95.10	87.63
BS-RH-PW 1:1:1-400 °C	125.00	126.47	98.84
BS-RH-PW 1:1:1-500 °C	125.00	195.10	64.07

Relative seed germination rate (RSGR), relative root growth (RRG), germination index (GI).

In biochars derived from BS pyrolysis, the GI increased with temperature, reaching values of 29%, 69%, and 58% at 300, 400, and 500 °C, respectively, with the highest value observed at 400 °C (see Table 6).

In contrast, the results for BS/RH co-pyrolysis exhibited an opposite trend: the GI decreased as the temperature rose. The highest values were recorded at 300 °C, with the BS/RH 2:1 biochar standing out at 86%, surpassing even the GI observed with BS pyrolysis. However, at 400 °C and 500 °C, the GI values decreased significantly, reaching minimum levels of 25–33% (see Table 6; Figure 11).

In contrast, the biochars derived from the co-pyrolysis of BS/PW exhibited a positive correlation with temperature, with significant increases in the GI at 400 °C, particularly in the BS/PW 1:2 mixture, which achieved a GI of 172%. At 500 °C, a slight decline was observed, although the GI values remained higher than those of the biochars produced exclusively from BSs (see Table 6). Germination index values exceeding 100% indicate a stimulatory effect on seed germination and early root development relative to the control and have been widely reported in phytotoxicity and biochar assessment studies as a response associated with improved nutrient availability, reduced phytotoxicity and favourable physicochemical conditions following biochar application [13,50,95–97].

Overall, the results indicate that the type of co-pyrolysed biomass exerts a differential influence on the GI. Specifically, the addition of RH promotes a higher GI at lower temperatures, while the inclusion of PW amplifies this effect at intermediate temperatures (400 °C). These findings suggest contrasting behaviours depending on the accompanying biomass.

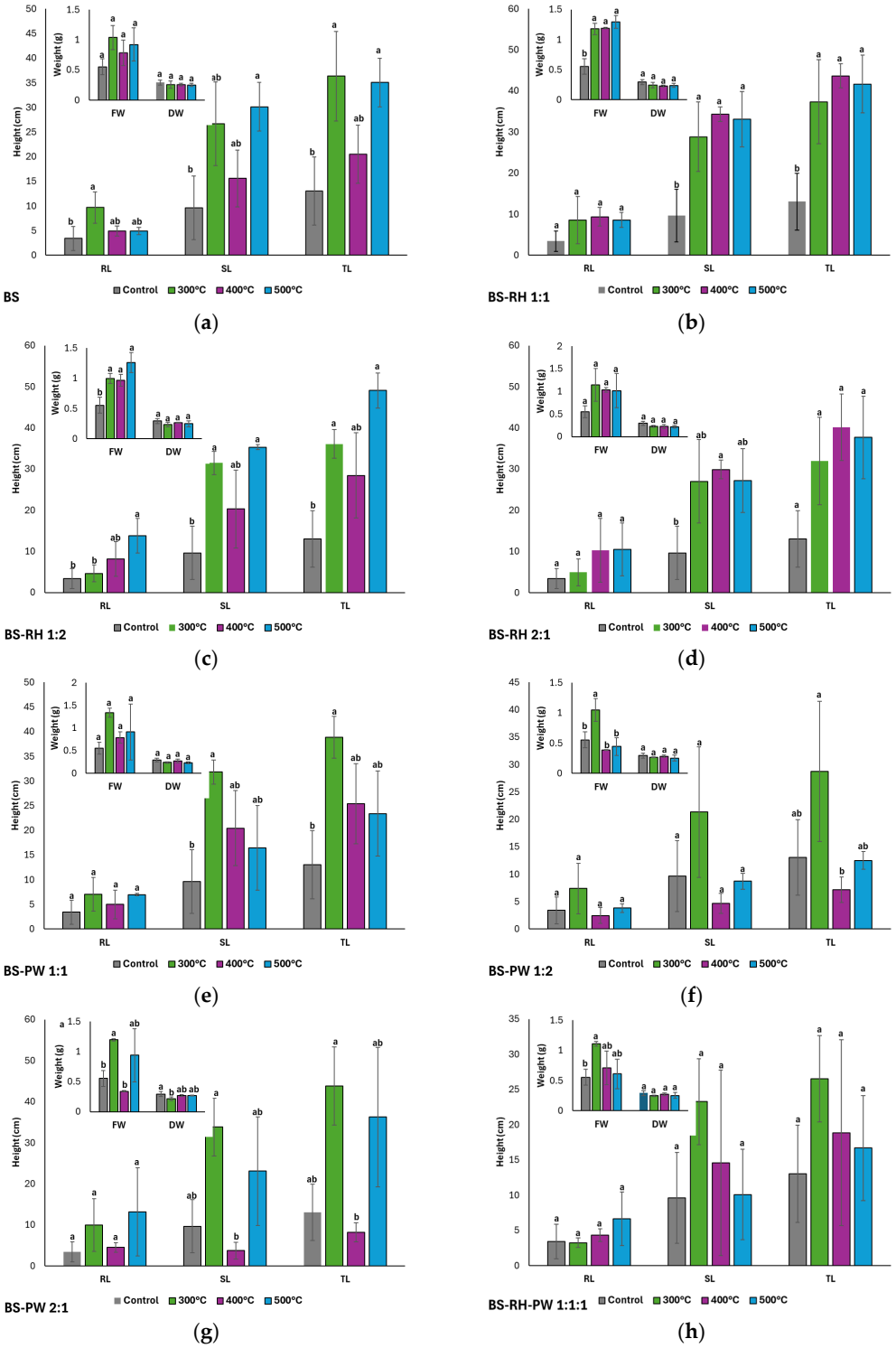

Figure 11. Physiological parameters from the germination assay using *Zea mays*. Each panel displays root length (RL), shoot length (SL), and total seedling length for each treatment enriched with biochar at pyrolysis temperatures of 300, 400, and 500 °C. The graphs of fresh weight (FW) and dry weight (DW) are located in the upper-left corner of each panel. Each panel corresponds to a specific biochar analysed in this study: (**a**) Biochar derived from BS pyrolysis, (**b**) Biochar from BS/RH 1:1 co-pyrolysis, (**c**) Biochar from BS/RH 1:2 co-pyrolysis, (**d**) Biochar from BS/RH 2:1 co-pyrolysis, (**e**) Biochar from BS/PW 1:1 co-pyrolysis, (**f**) Biochar from BS/PW 1:2 co-pyrolysis, (**g**) Biochar from BS/PW 2:1 co-pyrolysis, (**h**) Biochar from BS/RH/PW 1:1:1 co-pyrolysis. Different letters indicate statistically significant differences among treatments ($p < 0.05$).

As regards the aerial part (AP) of the seedlings, responses varied according to the biochar type. For biochar produced from BS alone, mean AP lengths were 26.67, 15.57, and 30.13 cm at 300, 400, and 500 °C, respectively, indicating a transient decline at 400 °C followed by recovery at 500 °C (Figure 11a).

Conversely, co-pyrolysis involving RH consistently yielded the highest AP values, demonstrating a general tendency to increase as the process temperature was elevated. Notably, the BS/RH 1:2 treatment at 500 °C recorded 35.33 cm (Figure 11c), which represents the maximum value obtained across all treatments in this study. In sharp contrast, co-pyrolysis with PW exhibited the opposite behaviour: AP generally decreased with rising temperature, reaching its minimum values at 400 °C and 500 °C. The only exception was the BS/PW 2:1 treatment (Figure 11g), which achieved a substantial 33.80 cm at the lower temperature of 300 °C.

Collectively, these results unequivocally demonstrate that the addition of RH consistently promoted greater above-ground development when compared to both BS pyrolysis alone and PW co-pyrolysis. This suggests a distinct positive effect of the RH co-substrate on the initial vegetative growth of maize.

Another critical parameter evaluated was the FW of the seedlings (Figure 11a). For the biochars obtained solely via BS pyrolysis, the FW values recorded were 1.04 g, 0.78 g, and 0.92 g at 300 °C, 400 °C, and 500 °C, respectively. Importantly, these figures all exceeded the FW of the control group.

In the co-pyrolysis treatments involving RH, a more pronounced positive effect was observed, generally demonstrating an increase in FW as the processing temperature was elevated. Specifically, the BS/RH 1:1 and BS/RH 1:2 treatments reached peak values of up to 1.29 g and 1.26 g at 500 °C, respectively. Conversely, the BS/RH 2:1 treatment remained relatively stable, consistently yielding FW values between 1.0 g and 1.1 g. In every instance of RH co-pyrolysis, the resulting FW values significantly surpassed those of the control (Figure 11b–d).

In contrast, co-pyrolysis involving PW demonstrated a distinct tendency for the FW of the seedlings to decrease as the process temperature increased. Although FW values at 300 °C were notably higher than the control (e.g., 1.34 g for BS/PW 1:1 and 1.19 g for BS/PW 2:1), a substantial reduction was observed at both 400 °C and 500 °C. This resulted in minimum FW values of 0.34 g and 0.39 g being recorded for the BS/PW 2:1and BS/PW 1:2 treatments, respectively (Figure 11e, f, and g).

Collectively, these results clearly indicate that the inclusion of RH consistently favoured an increase in the fresh weight of the seedlings. Conversely, the incorporation of PW had the opposite effect, significantly limiting seedling development, particularly when processed at elevated temperatures.

The GI is calculated as the product of the relative germination rate of the seed and the relative root growth. Consequently, high GI values indicate faster germination, whereas low values reflect greater root development. In the present study, co-pyrolysis with PW generated substantially higher GI values compared to co-pyrolysis with RH, suggesting a significant, positive effect on germination. Conversely, the addition of RH appeared to favour greater root elongation and, generally, an increase in the above-ground and fresh biomass of the resulting seedlings.

Overall, the results obtained clearly demonstrate that the incorporation of both RH and PW during co-pyrolysis with BSs induced distinct effects on maize growth. While co-pyrolysis with PW exhibited a tendency to stimulate germination, co-pyrolysis with RH distinctly promoted superior vegetative development, affecting both the AP and the total biomass. Both outcomes are considered favourable, as they could translate into valuable improvements in early crop establishment and subsequent potential yield.

3.5. Relationship Between the Variables of Biochars Derived from the Co-Pyrolysis of BSs

To investigate the relationships among the variables obtained from the characterisation of biochars derived from the pyrolysis of BSs and their co-pyrolysis with RH and PW, a PCA was performed. This analysis effectively integrated the complex dataset, allowing the distribution of the different treatment groups to be clearly visualised, which segregated into four distinct groups (Figure 12).

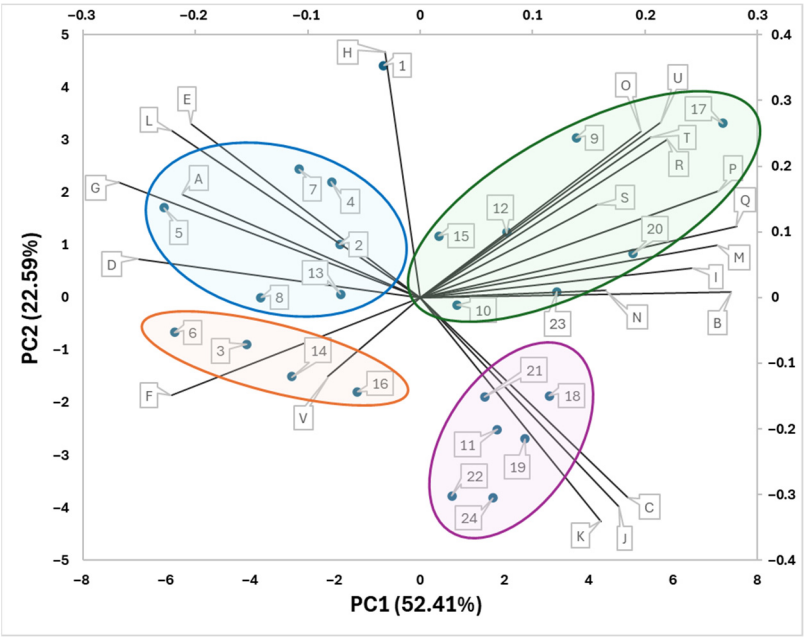

Figure 12. Principal Component Analysis of biochars produced by pyrolysis and co-pyrolysis of biosolids (BSs), rice husk (RH) and pruning waste (PW) at 300, 400 and 500 °C. Sample scores are identified by numerical codes corresponding to feedstock composition and pyrolysis temperature as follows: BS (1, 9, 17); BS–RH 1:1 (2, 10, 18); BS–RH 1:2 (3, 11, 19); BS–RH 2:1 (4, 12, 20); BS–PW 1:1 (5, 13, 21); BS–PW 1:2 (6, 14, 22); BS–PW 2:1 (7, 15, 23); and BS–RH–PW 1:1:1 (8, 16, 24), for 300, 400 and 500 °C, respectively. Variable loadings are denoted by letter codes: moisture (A), ash (B), pH (C), electrical conductivity (D), yield (E), C content (F), H content (G), N content (H), O content (I), specific surface area (J), pore volume (K), H/C atomic ratio (L), Al (M), Cr (N), Cu (O), Fe (P), K (Q), Mg (R), Ni (S), Pb (T), Zn (U), and germination index (V).

The green group, situated in the first quadrant, was distinguished by a higher percentage of ash and metal concentration. This observation was predictable, given that metals inherently tend to concentrate within the mineral fraction. This group primarily included biochars obtained at 400 °C and 500 °C, in both BS pyrolysis and co-pyrolysis with a higher BS proportion (2:1). This distribution confirms that elevated temperatures substantially favour the accumulation of the ash component.

In the blue group, located in the third quadrant, the variables humidity, electrical conductivity, yield, and the concentrations of H, N, and the H/C ratio predominated. The treatments corresponding to this group were primarily biochars produced at 300 °C with mass ratios of 1:1 and 2:1, both with RH and PW. These treatments were characterised by H/C ratios greater than 0.7, exceeding the values recommended in biochar certification standards.

The orange group was mainly associated with the carbon percentage and GI. In this group, treatments with a mass ratio of 1:2, where lignocellulosic biomass (predominantly PW) was present in higher quantities, were prominent. The temperatures of 300 °C and 400 °C showed a similar distribution, indicating that germination is positively correlated with the carbon content in the biochar, especially when PW constitutes a higher proportion.

The purple group, located in the fourth quadrant, was characterised by pH, surface area, and pore volume. This group was primarily composed of biochars obtained at 500 °C, predominantly derived from pyrolysis with RH (60%) and mainly with a 1:2 mass ratio. These results suggest that the addition of RH enhances the surface and chemical properties of biochar, including pH, surface area, and porosity.

The grouping of biochars into different quadrants through PCA aids in identifying their potential applications. In terms of soil amendment, biochars from the orange and purple groups are the most promising, owing to their higher carbon content, better germination performance (particularly in the case of PW), and superior surface and chemical properties (especially in the case of RH). In contrast, biochars from the green and blue groups have certain limitations: the green group is hindered by its higher ash and heavy metal content, while the blue group exceeds the recommended H/C ratio limits set by international certification standards.

Overall, the PCA highlights that PW biomass improves biological parameters such as germination rate and carbon content, while RH biomass enhances physicochemical properties like surface area, pore volume, and pH, key factors for their application in agricultural systems.

4. Conclusions

In this study, biochars derived from the pyrolysis of BSs, along with their co-pyrolysis with RH and PW, were produced and characterised. The results revealed that co-pyrolysis significantly enhanced the properties of the biochars compared to those generated exclusively from BSs. The incorporation of PW increased the carbon content, while RH contributed to improvements in surface area, pore size, and pH, all of which are critical factors for agricultural applications.

Both the pyrolysis temperature and the mass ratio used had a significant impact on the final properties of the biochars. The most favourable conditions were observed at 1:2 ratios (BS/PW and BS/RH) at pyrolysis temperatures of 400 °C and 500 °C. Under these conditions, key attributes such as porosity, surface area, electrical conductivity, and pH were optimised. These findings present promising avenues for future research into the application of biochars in soil enhancement.

However, the presence of HM remains a significant limitation. While a dilution effect was noted, particularly in the case of PW, the chemical fractions containing HMs were not analysed, which limits an understanding of their bioavailability and potential environmental risks. It is recommended that both short- and long-term studies continue, focusing on the mobility of HMs in the soil–biochar–plant interaction to better assess their environmental impact.

In summary, this study definitively demonstrates that the co-pyrolysis of BSs with agro-forestry biomass constitutes an effective strategy for enhancing the physicochemical quality of the resulting biochars. This process not only yields a valuable product but also represents a sustainable alternative for the integrated management and valorisation of BSs. However, for the widespread agricultural application of these biochars, compliance with established international certification parameters (e.g., those set by the IBI and EBC) remains paramount. Furthermore, there is an urgent need to expedite the creation of robust national standards that specifically account for the unique characteristics of BSs generated within Mexico. Adopting these measures will significantly strengthen the commercial viability of biochar as a soil amendment and secure its role as a crucial tool for integrated waste management.

Author Contributions: Conceptualization, L.M.L.-Z., O.S.C.-B., M.d.l.L.X.N.-R. and E.C.-B.; methodology, L.M.L.-Z., C.A.R.-V., M.d.l.L.X.N.-R., H.P.-G., D.A.R.-A., D.Á.-B., M.A.L.-H. and E.C.-B.; software, O.S.C.-B., D.A.R.-A. and E.C.-B.; validation, L.M.L.-Z., O.S.C.-B. and E.C.-B.; formal analysis L.M.L.-Z., O.S.C.-B. and E.C.-B.; investigation, L.M.L.-Z., H.P.-G. and C.A.R.-V.; resources, L.M.L.-Z., C.A.R.-V., H.P.-G. and C.L.-P.; data curation, L.M.L.-Z., C.A.R.-V., C.L.-P., D.A.R.-A. and O.S.C.-B.; writing—original draft preparation L.M.L.-Z., O.S.C.-B., M.d.l.L.X.N.-R. and E.C.-B.; writing—review and editing, L.M.L.-Z., O.S.C.-B., M.d.l.L.X.N.-R. and E.C.-B. visualization, L.M.L.-Z. and O.S.C.-B.; supervision, E.C.-B.; project administration, L.M.L.-Z., C.A.R.-V. and E.C.-B. All authors have read and agreed to the published version of the manuscript.

Funding: This research was funded by a SECIHTI postgraduate scholarship (Grant No. 2023-000002-01NACF-02843) and by the Tecnológico Nacional de México, Celaya Campus, under project grant CELA-PYR-2025-22576.

Institutional Review Board Statement: Not applicable.

Informed Consent Statement: Not applicable.

Data Availability Statement: The original contributions presented in this study are included in the article. Further inquiries can be directed to the corresponding author.

Acknowledgments: We are grateful to the Centro de Investigación en Materiales Avanzados (CIMAV) for providing facilities for the research stay and for enabling the characterisation techniques, including elemental analysis, heavy-metal quantification, BET analysis and SEM–EDS. We especially acknowledge the support of Alejandro Benavides Montoya, Flor Griselda Nevárez Vargas, Claudia Patricia Peregrino Ibarra and Manuel Román, from CIMAV, for their work on characterisation methodologies. We thank the Laboratorio de Termofluidos of the Universidad de Guanajuato (UG), Irapuato–Salamanca Campus, for facilitating the production of biochars. We are grateful to Eng. Julio César Toche Flores, Manager of the Urban Wastewater Treatment Plant (PTARU) of Celaya, Gto., Mexico, for support with BS sampling. We also thank the Dirección Municipal de Medio Ambiente of Celaya, Gto., Mexico, for assistance in obtaining PW. We acknowledge the UG, Celaya–Salvatierra Campus (Mutualismo site), for providing facilities to conduct *Zea mays* germination tests. Finally, we thank the Laboratorio de Biotecnología Ambiental y Bioprocesos of the Tecnológico Nacional de México (TecNM) in Celaya for the availability of its facilities for the development of this project and for the equipment provided for the characterisation of biochars.

Conflicts of Interest: The authors declare no conflict of interest.

Abbreviations

The following abbreviations are used in this manuscript:

Al	Aluminium	AP	Aerial Part
AS	Activated Sludge	BET	Brunauer–Emmett–Teller
BSs	Biosolids	C	Carbon
Cd	Cadmium	Cr	Chromium
CS	Cotton Stalks	Cu	Copper
DW	Dry Weight	EBC	European Biochar Certificate
EC	Electrical Conductivity	EDS	Energy Dispersive Spectroscopy
EU	European Union	Fe	Iron
FTIR	Fourier Transform Infrared Spectroscopy	FW	Fresh Weight
GI	Germination Index	H	Hydrogen
H/C	Atomic Hydrogen to Organic Carbon Ratio	HMs	Heavy Metals
IBI	International Biochar Initiative	K	Potassium
Mg	Magnesium	MSS	Municipal Sewage Sludge

N	Nitrogen	Na	Sodium
Ni	Nickel	P	Phosphorus
Pb	Lead	PCA	Principal Component Analysis
pH	Hydrogen Potential	PW	Pruning Waste
Rc	Average Root Length in the Control	RH	Rice Husk
RL	Root Length	RRG	Relative Root Growth
RS	Rice Straw	Rs	Average Root Length in the Sample
RSGR	Relative Seed Germination Rate	S	Sulfur
Sc	Seeds Germinated in the Control	SD	Sawdust
SEM	Scanning Electron Microscopy	Si	Silicon
SL	Shoot Length	Ss	Seeds Germinated in the Sample
SS	Sewage Sludge	TL	Total Length
USA	United States of America	Zn	Zinc

References

1. Fan, Z.; Zhou, X.; Peng, Z.; Wan, S.; Gao, Z.F.; Deng, S.; Tong, L.; Han, W.; Chen, X. Co-pyrolysis technology for enhancing the functionality of sewage sludge biochar and immobilizing heavy metals. *Chemosphere* **2023**, *317*, 137929. [CrossRef] [PubMed]
2. Wang, X.; Chang, V.W.-C.; Li, Z.; Chen, Z.; Wang, Y. Co-pyrolysis of sewage sludge and organic fractions of municipal solid waste: Synergistic effects on biochar properties and the environmental risk of heavy metals. *J. Hazard. Mater.* **2021**, *412*, 125200. [CrossRef] [PubMed]
3. Paz-Ferreiro, J.; Nieto, A.; Méndez, A.; Askeland, M.P.J.; Gascó, G. Biochar from Biosolids Pyrolysis: A Review. *Int. J. Environ. Res. Public Health* **2018**, *15*, 956. [CrossRef] [PubMed]
4. Smith, K.M.; Fowler, G.D.; Pullket, S.; Graham, N.J.D. Sewage sludge-based adsorbents: A review of their production, properties and use in water treatment applications. *Water Res.* **2009**, *43*, 2569–2594. [CrossRef]
5. Wang, Z.; Wang, J.; Xie, L.; Zhu, H.; Shu, X. Influence of the Addition of Cotton Stalk during Co-pyrolysis with Sewage Sludge on the Properties, Surface Characteristics, and Ecological Risks of Biochars. *J. Therm. Sci.* **2019**, *28*, 755–762. [CrossRef]
6. Biney, M.; Gusiatin, M.Z. Biochar from Co-Pyrolyzed Municipal Sewage Sludge (MSS): Part 1: Evaluating Types of Co-Substrates and Co-Pyrolysis Conditions. *Materials* **2024**, *17*, 3603. [CrossRef]
7. Biney, M.; Gusiatin, M.Z. Biochar from Co-Pyrolyzed Municipal Sewage Sludge (MSS): Part 2: Biochar Characterization and Application in the Remediation of Heavy Metal-Contaminated Soils. *Materials* **2024**, *17*, 3850. [CrossRef]
8. Chen, Q.; Liu, H.; Ko, J.; Wu, H.; Xu, Q. Structure characteristics of bio-char generated from co-pyrolysis of wooden waste and wet municipal sewage sludge. *Fuel Process. Technol.* **2019**, *183*, 48–54. [CrossRef]
9. Yang, Y.Q.; Cui, M.H.; Guo, J.C.; Du, J.J.; Zheng, Z.Y.; Liu, H. Effects of co-pyrolysis of rice husk and sewage sludge on the bioavailability and environmental risks of Pb and Cd. *Environ. Technol.* **2021**, *42*, 2304–2312. [CrossRef]
10. International Biochar Initiative. 2023. Available online: https://biocharinternational.org/ (accessed on 25 September 2023).
11. Novotný, M.; Marković, M.; Raček, J.; Šipka, M.; Chorazy, T.; Tošić, I.; Hlavínek, P. The use of biochar made from biomass and biosolids as a substrate for green infrastructure: A review. *Sustain. Chem. Pharm.* **2023**, *32*, 100999. [CrossRef]
12. Urbina-Salas, I.; Granados-Lieberman, D.; Valtierra-Rodríguez, M.; Ramírez-Valdespino, C.A.; Rodríguez-Alejandro, D.A. Modeling of Global and Individual Kinetic Parameters in Wheat Straw Torrefaction: Particle Swarm Optimization and Its Impact on Elemental Composition Prediction. *Algorithms* **2025**, *18*, 283. [CrossRef]
13. Huang, H.J.; Yang, T.; Lai, F.Y.; Wu, G.Q. Co-pyrolysis of sewage sludge and sawdust/rice straw for the production of biochar. *J. Anal. Appl. Pyrolysis* **2017**, *125*, 61–68. [CrossRef]
14. Standard Test Method for Ash in Wood. Available online: https://www.astm.org/d1102-84r21.html (accessed on 15 April 2024).
15. Standard Test Method for Moisture Analysis of Particulate Wood Fuels. Available online: https://www.astm.org/e0871-82r19.html (accessed on 15 April 2024).
16. Standard Test Method for Volatile Matter in the Analysis of Particulate Wood Fuels. Available online: https://www.astm.org/e0872-82r19.html (accessed on 15 April 2024).
17. Wang, J.; Wang, S. Preparation, modification and environmental application of biochar: A review. *J. Clean. Prod.* **2019**, *227*, 1002–1022. [CrossRef]
18. Gbouri, I.; Yu, F.; Wang, X.; Wang, J.; Cui, X.; Hu, Y.; Yan, B.; Chen, G. Co-Pyrolysis of Sewage Sludge and Wetland Biomass Waste for Biochar Production: Behaviors of Phosphorus and Heavy Metals. *Int. J. Environ. Res. Public Health* **2022**, *19*, 2818. [CrossRef]
19. Rajkovich, S.; Enders, A.; Hanley, K.; Hyland, C.; Zimmerman, A.R.; Lehmann, J. Corn growth and nitrogen nutrition after additions of biochars with varying properties to a temperate soil. *Biol. Fertil. Soils* **2012**, *48*, 271–284. [CrossRef]

20. Patiño-Galván, H.; Bedolla-Rivera, H.I.; Negrete-Rodríguez, M.d.l.L.X.; Herrera-Pérez, A.; Álvarez-Bernal, D.; Lastiri-Hernández, M.A.; Bernardino-Nicanor, A.; González-Cruz, L.; Conde-Barajas, E. Effects of Microplastics from Face Masks on Physicochemical and Biological Properties of Agricultural Soil: Development of Soil Quality Index "SQI". *Appl. Sci.* **2025**, *15*, 2010. [CrossRef]
21. Wang, Z.; Shu, X.; Zhu, H.; Xie, L.; Cheng, S.; Zhang, Y. Characteristics of biochars prepared by co-pyrolysis of sewage sludge and cotton stalk intended for use as soil amendments. *Environ. Technol.* **2018**, *41*, 1347–1357. [CrossRef]
22. Van Zwieten, L.; Kimber, S.; Morris, S.; Chan, K.Y.; Downie, A.; Rust, J.; Joseph, S.; Cowie, A. Effects of biochar from slow pyrolysis of papermill waste on agronomic performance and soil fertility. *Plant Soil.* **2010**, *327*, 235–246. [CrossRef]
23. Ahmad, A.; Chowdhary, P.; Khan, N.; Chaurasia, D.; Varjani, S.; Pandey, A.; Chaturvedi, P. Effect of sewage sludge biochar on the soil nutrient, microbial abundance, and plant biomass: A sustainable approach towards mitigation of solid waste. *Chemosphere* **2022**, *287*, 132112. [CrossRef]
24. de Figueiredo, C.C.; Chagas, J.K.M.; da Silva, J.; Paz-Ferreiro, J. Short-term effects of a sewage sludge biochar amendment on total and available heavy metal content of a tropical soil. *Geoderma* **2019**, *344*, 31–39. [CrossRef]
25. Thomas, G.W. *Soil pH and Soil Acidity*; Sparks, D.L., Page, A.L., Helmke, P.A., Loeppert, R.H., Soltanpour, P.N., Tabatabai, M.A., Johnston, C.T., Sumner, M.E., Eds.; SSSA Book Series; Soil Science Society of America, American Society of Agronomy: Madison, WI, USA, 2018; pp. 475–490. Available online: http://doi.wiley.com/10.2136/sssabookser5.3.c16 (accessed on 2 July 2025).
26. Hendrickx, J.M.H.; Borchers, B.; Corwin, D.L.; Lesch, S.M.; Hilgendorf, A.C.; Schlue, J. Inversion of Soil Conductivity Profiles from Electromagnetic Induction Measurements. *Soil. Sci. Soc. Am. J.* **2002**, *66*, 673–685.
27. Das, P.; Bahadur, N.; Dhawan, V. Surfactant-modified titania for cadmium removal and textile effluent treatment together being environmentally safe for seed germination and growth of Vigna radiata. *Environ. Sci. Pollut. Res.* **2020**, *27*, 7795–7811. [CrossRef] [PubMed]
28. Guzmán-Maldonado, S.H.; López-Manzano, M.J.; Madera-Santana, T.J.; Núñez-Colín, C.A.; Grijalva-Verdugo, C.P.; Villa-Lerma, A.G.; Rodríguez-Núñez, J.R. Nutritional characterization of Moringa oleífera leaves, seeds, husks and flowers from two regions of Mexico. *Agron. Colomb.* **2020**, *38*, 287–297. [CrossRef]
29. Johnson, D.E. *Métodos Multivariados Aplicados al Análisis de Datos*; Internacional Thomson Ed: México City, Mexico, 2000; 566p.
30. Núñez-Colín, C.A.; Escobedo-López, D. Caracterización de germoplasma vegetal: La piedra angular en el estudio de los recursos fitogenéticos. *Acta Agrícola Pecu.* **2014**, *1*, 1–6.
31. Weber, K.; Quicker, P. Properties of biochar. *Fuel* **2018**, *217*, 240–261. [CrossRef]
32. Yang, Y.Q.; Cui, M.H.; Ren, Y.G.; Guo, J.C.; Zheng, Z.Y.; Liu, H. Towards Understanding the Mechanism of Heavy Metals Immobilization in Biochar Derived from Co-pyrolysis of Sawdust and Sewage Sludge. *Bull. Environ. Contam. Toxicol.* **2020**, *104*, 489–496. [CrossRef] [PubMed]
33. Xu, X.; Zhao, B.; Sun, M.; Chen, X.; Zhang, M.; Li, H.; Xu, S. Co-pyrolysis characteristics of municipal sewage sludge and hazelnut shell by TG-DTG-MS and residue analysis. *Waste Manag.* **2017**, *62*, 91–100. [CrossRef]
34. Hossain, M.K.; Strezov, V.; Chan, K.Y.; Ziolkowski, A.; Nelson, P.F. Influence of pyrolysis temperature on production and nutrient properties of wastewater sludge biochar. *J. Environ. Manag.* **2011**, *92*, 223–228. [CrossRef]
35. Zhang, J.; Lü, F.; Zhang, H.; Shao, L.; Chen, D.; He, P. Multiscale visualization of the structural and characteristic changes of sewage sludge biochar oriented towards potential agronomic and environmental implication. *Sci. Rep.* **2015**, *5*, 9406. [CrossRef]
36. Zabaniotou, A.; Stamou, K. Balancing Waste and Nutrient Flows Between Urban Agglomerations and Rural Ecosystems: Biochar for Improving Crop Growth and Urban Air Quality in The Mediterranean Region. *Atmosphere* **2020**, *11*, 539. [CrossRef]
37. El-Naggar, A.; Lee, S.S.; Rinklebe, J.; Farooq, M.; Song, H.; Sarmah, A.K.; Zimmerman, A.R.; Ahmad, M.; Shaheen, S.M.; Ok, Y.S. Biochar application to low fertility soils: A review of current status, and future prospects. *Geoderma* **2019**, *337*, 536–554. [CrossRef]
38. Glaser, B.; Lehmann, J.; Zech, W. Ameliorating physical and chemical properties of highly weathered soils in the tropics with charcoal–a review. *Biol. Fertil. Soils* **2002**, *35*, 219–230. [CrossRef]
39. Kookana, R.S.; Sarmah, A.K.; Van Zwieten, L.; Krull, E.; Singh, B. *Chapter Three-Biochar Application to Soil: Agronomic and Environmental Benefits and Unintended Consequences; Advances in Agronomy*; Sparks, D.L., Ed.; Academic Press: Cambridge, MA, USA, 2011; pp. 103–143. Available online: https://www.sciencedirect.com/science/article/pii/B9780123855381000032 (accessed on 8 July 2025).
40. Major, J.; Rondon, M.; Molina, D.; Riha, S.J.; Lehmann, J. Maize yield and nutrition during 4 years after biochar application to a Colombian savanna oxisol. *Plant Soil.* **2010**, *333*, 117–128. [CrossRef]
41. Raboin, L.M.; Razafimahafaly, A.H.D.; Rabenjarisoa, M.B.; Rabary, B.; Dusserre, J.; Becquer, T. Improving the fertility of tropical acid soils: Liming versus biochar application? A long term comparison in the highlands of Madagascar. *Field Crops Res.* **2016**, *199*, 99–108. [CrossRef]
42. Rinklebe, J.; Shaheen, S.M.; Frohne, T. Amendment of biochar reduces the release of toxic elements under dynamic redox conditions in a contaminated floodplain soil. *Chemosphere* **2016**, *142*, 41–47. [CrossRef]
43. Zhang, R.; Zhang, Y.; Song, L.; Song, X.; Hänninen, H.; Wu, J. Biochar enhances nut quality of Torreya grandis and soil fertility under simulated nitrogen deposition. *For. Ecol. Manag.* **2017**, *391*, 321–329. [CrossRef]

44. Laghari, M.; Mirjat, M.S.; Hu, Z.; Fazal, S.; Xiao, B.; Hu, M.; Chen, Z.; Guo, D. Effects of biochar application rate on sandy desert soil properties and sorghum growth. *CATENA* **2015**, *135*, 313–320. [CrossRef]
45. Lentz, R.D.; Ippolito, J.A. Biochar and Manure Affect Calcareous Soil and Corn Silage Nutrient Concentrations and Uptake. *J. Environ. Qual.* **2012**, *41*, 1033–1043. [CrossRef]
46. Wang, T.; Chen, Y.; Li, J.; Xue, Y.; Liu, J.; Mei, M.; Hou, H.; Chen, S. Co-pyrolysis behavior of sewage sludge and rice husk by TG-MS and residue analysis. *J. Clean. Prod.* **2020**, *250*, 119557. [CrossRef]
47. Kalina, M.; Sovova, S.; Svec, J.; Trudicova, M.; Hajzler, J.; Kubikova, L.; Enev, V. The Effect of Pyrolysis Temperature and the Source Biomass on the Properties of Biochar Produced for the Agronomical Applications as the Soil Conditioner. *Materials* **2022**, *15*, 8855. [CrossRef]
48. Ali, L.; Palamanit, A.; Techato, K.; Ullah, A.; Chowdhury, M.S.; Phoungthong, K. Characteristics of Biochars Derived from the Pyrolysis and Co-Pyrolysis of Rubberwood Sawdust and Sewage Sludge for Further Applications. *Sustainability* **2022**, *14*, 3829. [CrossRef]
49. Khanmohammadi, Z.; Afyuni, M.; Mosaddeghi, M.R. Effect of pyrolysis temperature on chemical and physical properties of sewage sludge biochar. *Waste Manag. Res.* **2015**, *33*, 275–283. [CrossRef] [PubMed]
50. Raj, A.; Yadav, A.; Arya, S.; Sirohi, R.; Kumar, S.; Rawat, A.P.; Thakur, R.S.; Patel, D.K.; Bahadur, L.; Pandey, A. Preparation, characterization and agri applications of biochar produced by pyrolysis of sewage sludge at different temperatures. *Sci. Total Environ.* **2021**, *795*, 148722. [CrossRef] [PubMed]
51. Agrafioti, E.; Bouras, G.; Kalderis, D.; Diamadopoulos, E. Biochar production by sewage sludge pyrolysis. *J. Anal. Appl. Pyrolysis* **2013**, *101*, 72–78. [CrossRef]
52. Han, L.; Li, J.; Qu, C.; Shao, Z.; Yu, T.; Yang, B. Recent Progress in Sludge Co-Pyrolysis Technology. *Sustainability* **2022**, *14*, 7574. [CrossRef]
53. Mohamed, B.A.; Ruan, R.; Bilal, M.; Khan, N.A.; Awasthi, M.K.; Amer, M.A.; Leng, L.; Hamouda, M.A.; Vo, D.N.; Li, J. Co-pyrolysis of sewage sludge and biomass for stabilizing heavy metals and reducing biochar toxicity: A review. *Environ. Chem. Lett.* **2023**, *21*, 1231–1250. [CrossRef]
54. Ok, Y.S.; Uchimiya, S.M.; Chang, S.X.; Bolan, N. (Eds.) *Biochar: Production, Characterization, and Applications*; CRC Press: Boca Raton, FL, USA, 2015; 438p.
55. Warnock, D.D.; Lehmann, J.; Kuyper, T.W.; Rillig, M.C. Mycorrhizal responses to biochar in soil–concepts and mechanisms. *Plant Soil.* **2007**, *300*, 9–20. [CrossRef]
56. Sharma, B.; Sarkar, A.; Singh, P.; Singh, R.P. Agricultural utilization of biosolids: A review on potential effects on soil and plant grown. *Waste Manag.* **2017**, *64*, 117–132. [CrossRef]
57. Medina-Herrera, M.d.R.; Negrete-Rodríguez, M.d.l.L.X.; Álvarez-Trejo, J.L.; Samaniego-Hernández, M.; González-Cruz, L.; Bernardino-Nicanor, A.; Conde-Barajas, E. Evaluation of Non-Conventional Biological and Molecular Parameters as Potential Indicators of Quality and Functionality of Urban Biosolids Used as Organic Amendments of Agricultural Soils. *Appl. Sci.* **2020**, *10*, 517. [CrossRef]
58. Hossain, Z.; Bahar, M.; Sarkar, B.; Donne, S.W.; Ok, Y.S.; Palansooriya, K.N.; Kirkham, M.B.; Chowdhury, S.; Bolan, N. Biochar and its importance on nutrient dynamics in soil and plant. *Biochar* **2020**, *2*, 379–420. [CrossRef]
59. Knicker, H. "Black nitrogen"–an important fraction in determining the recalcitrance of charcoal. *Org. Geochem.* **2010**, *41*, 947–950. [CrossRef]
60. Knicker, H.; Hilscher, A.; González-Vila, F.J.; Almendros, G. A new conceptual model for the structural properties of char produced during vegetation fires. *Org. Geochem.* **2008**, *39*, 935–939. [CrossRef]
61. Paneque, M.; De la Rosa, J.M.; Kern, J.; Reza, M.T.; Knicker, H. Hydrothermal carbonization and pyrolysis of sewage sludges: What happen to carbon and nitrogen? *J. Anal. Appl. Pyrolysis* **2017**, *128*, 314–323. [CrossRef]
62. de la Rosa, J.M.; Knicker, H. Bioavailability of N released from N-rich pyrogenic organic matter: An incubation study. *Soil. Biol. Biochem.* **2011**, *43*, 2368–2373. [CrossRef]
63. Chen, J.; Wang, P.; Ding, L.; Yu, T.; Leng, S.; Chen, J.; Fan, L.; Li, J.; Wei, L.; Li, J.; et al. The comparison study of multiple biochar stability assessment methods. *J. Anal. Appl. Pyrolysis* **2021**, *156*, 105070. [CrossRef]
64. The European Biochar Certificate (EBC). Available online: https://www.european-biochar.org/en (accessed on 19 March 2025).
65. Xiao, X.; Chen, Z.; Chen, B. H/C atomic ratio as a smart linkage between pyrolytic temperatures, aromatic clusters and sorption properties of biochars derived from diverse precursory materials. *Sci. Rep.* **2016**, *6*, 22644. [CrossRef]
66. Amalina, F.; Syukor Abd Razak, A.; Krishnan, S.; Sulaiman, H.; Zularisam, A.W.; Nasrullah, M. Advanced techniques in the production of biochar from lignocellulosic biomass and environmental applications. *Clean. Mater.* **2022**, *6*, 100137. [CrossRef]
67. Lee, J.W.; Kidder, M.; Evans, B.R.; Paik, S.; Iii, A.C.B.; Garten, C.T.; Brown, R.C. Characterization of biochars produced from cornstovers for soil amendment. *Environ. Sci. Technol.* **2010**, *44*, 7970–7974. [CrossRef]

68. Ali, S.; Rizwan, M.; Qayyum, M.F.; Ok, Y.S.; Ibrahim, M.; Arif, M.S.; Hafeez, F.; Al-Wabel, M.I.; Shahzad, A.N. Biochar soil amendment on alleviation of drought and salt stress in plants: A critical review. *Environ. Sci. Pollut. Res.* **2017**, *24*, 12700–12712. [CrossRef]
69. Brickler, C.A.; Wu, Y.; Li, S.; Anandhi, A.; Chen, G. Comparing Physicochemical Properties and Sorption Behaviors of Pyrolysis-Derived and Microwave-Mediated Biochar. *Sustainability* **2021**, *13*, 2359. [CrossRef]
70. Sun, Y.; Xiong, X.; He, M.; Xu, Z.; Hou, D.; Zhang, W.; Ok, Y.S.; Rinklebe, J.; Wang, L.; Tsang, D.C. Roles of biochar-derived dissolved organic matter in soil amendment and environmental remediation: A critical review. *Chem. Eng. J.* **2021**, *424*, 130387. [CrossRef]
71. Beusch, C. Biochar as a Soil Ameliorant: How Biochar Properties Benefit Soil Fertility—A Review. *J. Geosci. Environ. Prot.* **2021**, *9*, 28–46. [CrossRef]
72. Wang, X.; Li, C.; Zhang, B.; Lin, J.; Chi, Q.; Wang, Y. Migration and risk assessment of heavy metals in sewage sludge during hydrothermal treatment combined with pyrolysis. *Bioresour. Technol.* **2016**, *221*, 560–567. [CrossRef] [PubMed]
73. Wang, X.; Wei-Chung Chang, V.; Li, Z.; Song, Y.; Li, C.; Wang, Y. Co-pyrolysis of sewage sludge and food waste digestate to synergistically improve biochar characteristics and heavy metals immobilization. *Waste Manag.* **2022**, *141*, 231–239. [CrossRef] [PubMed]
74. Aksoy, C.; Severcan, F. Role of Vibrational Spectroscopy in Stem Cell Research. *J. Spectrosc.* **2012**, *27*, 513286. [CrossRef]
75. El Fels, L.; Zamama, M.; El Asli, A.; Hafidi, M. Assessment of biotransformation of organic matter during co-composting of sewage sludge-lignocelullosic waste by chemical, FTIR analyses, and phytotoxicity tests. *Int. Biodeterior. Biodegrad.* **2014**, *87*, 128–137. [CrossRef]
76. Tandy, S.; Healey, J.R.; Nason, M.A.; Williamson, J.C.; Jones, D.L.; Thain, S.C. FT-IR as an alternative method for measuring chemical properties during composting. *Bioresour. Technol.* **2010**, *101*, 5431–5436. [CrossRef]
77. Zhang, J.; Lü, F.; Shao, L.; He, P. The use of biochar-amended composting to improve the humification and degradation of sewage sludge. *Bioresour. Technol.* **2014**, *168*, 252–258. [CrossRef]
78. Zhou, Y.; Selvam, A.; Wong, J.W.C. Evaluation of humic substances during co-composting of food waste, sawdust and Chinese medicinal herbal residues. *Bioresour. Technol.* **2014**, *168*, 229–234. [CrossRef]
79. Lü, F.; Shao, L.-M.; Zhang, H.; Fu, W.-D.; Feng, S.-J.; Zhan, L.-T.; Chen, Y.-M.; He, P.-J. Application of advanced techniques for the assessment of bio-stability of biowaste-derived residues: A minireview. *Bioresour. Technol.* **2018**, *248*, 122–133. [CrossRef]
80. Soobhany, N.; Gunasee, S.; Rago, Y.P.; Joyram, H.; Raghoo, P.; Mohee, R.; Garg, V.K. Spectroscopic, thermogravimetric and structural characterization analyses for comparing Municipal Solid Waste composts and vermicomposts stability and maturity. *Bioresour. Technol.* **2017**, *236*, 11–19. [CrossRef] [PubMed]
81. Ghorbani, M.; Asadi, H.; Abrishamkesh, S. Effects of rice husk biochar on selected soil properties and nitrate leaching in loamy sand and clay soil. *Int. Soil. Water Conserv. Res.* **2019**, *7*, 258–265. [CrossRef]
82. Wang, X.; Li, C.; Li, Z.; Yu, G.; Wang, Y. Effect of pyrolysis temperature on characteristics, chemical speciation and risk evaluation of heavy metals in biochar derived from textile dyeing sludge. *Ecotoxicol. Environ. Saf.* **2019**, *168*, 45–52. [CrossRef] [PubMed]
83. Ding, Y.; Liu, Y.; Liu, S.; Li, Z.; Tan, X.; Huang, X.; Zeng, G.; Zhou, L.; Zheng, B. Biochar to improve soil fertility. A review. *Agron. Sustain. Dev.* **2016**, *36*, 36. [CrossRef]
84. Li, J.; Yu, G.; Pan, L.; Li, C.; You, F.; Xie, S.; Wang, Y.; Ma, J.; Shang, X. Study of ciprofloxacin removal by biochar obtained from used tea leaves. *J. Environ. Sci.* **2018**, *73*, 20–30. [CrossRef]
85. Jin, J.; Li, Y.; Zhang, J.; Wu, S.; Cao, Y.; Liang, P.; Zhang, J.; Wong, M.H.; Wang, M.; Shan, S.; et al. Influence of pyrolysis temperature on properties and environmental safety of heavy metals in biochars derived from municipal sewage sludge. *J. Hazard. Mater.* **2016**, *320*, 417–426. [CrossRef]
86. Kalina, M.; Sovova, S.; Hajzler, J.; Kubikova, L.; Trudicova, M.; Smilek, J.; Enev, V. Biochar Texture—A Parameter Influencing Physicochemical Properties, Morphology, and Agronomical Potential. *Agronomy* **2022**, *12*, 1768. [CrossRef]
87. Xiong, Q.; Wu, X.; Lv, H.; Liu, S.; Hou, H.; Wu, X. Influence of rice husk addition on phosphorus fractions and heavy metals risk of biochar derived from sewage sludge. *Chemosphere* **2021**, *280*, 130566. [CrossRef]
88. Ogunremi, O.O.; Ogunkunle, C.O.; Fatoba, P.O. Characterization and Remediation Potential of Sorghum and Rice Straw-Derived Biochars on Incubated Spent-Oil Contaminated Soil. *Sci. Afr.* **2023**, *22*, e01921. [CrossRef]
89. Lu, S.; Zong, Y. Pore structure and environmental serves of biochars derived from different feedstocks and pyrolysis conditions. *Environ. Sci. Pollut. Res.* **2018**, *25*, 30401–30409. [CrossRef]
90. Yin, Q.; Liu, M.; Ren, H. Biochar produced from the co-pyrolysis of sewage sludge and walnut shell for ammonium and phosphate adsorption from water. *J. Environ. Manag.* **2019**, *249*, 109410. [CrossRef]
91. Jin, F.; Ran, C.; Anwari, Q.A.; Geng, Y.Q.; Guo, L.Y.; Li, J.B.; Han, D.; Zhang, X.Q.; Liu, X.; Shao, X.W. Effects of biochar on sodium ion accumulation, yield and quality of rice in saline-sodic soil of the west of Songnen plain, northeast China. *Plant Soil. Environ.* **2018**, *64*, 612–618. [CrossRef]

92. Jin, J.; Wang, M.; Cao, Y.; Wu, S.; Liang, P.; Li, Y.; Zhang, J.; Zhang, J.; Wong, M.H.; Shan, S.; et al. Cumulative effects of bamboo sawdust addition on pyrolysis of sewage sludge: Biochar properties and environmental risk from metals. *Bioresour. Technol.* **2017**, *228*, 218–226. [CrossRef]
93. Shi, W.; Liu, C.; Shu, Y.; Feng, C.; Lei, Z.; Zhang, Z. Synergistic effect of rice husk addition on hydrothermal treatment of sewage sludge: Fate and environmental risk of heavy metals. *Bioresour. Technol.* **2013**, *149*, 496–502. [CrossRef] [PubMed]
94. Hu, J.; Zhao, L.; Luo, J.; Gong, H.; Zhu, N. A sustainable reuse strategy of converting waste activated sludge into biochar for contaminants removal from water: Modifications, applications and perspectives. *J. Hazard. Mater.* **2022**, *438*, 129437. [CrossRef] [PubMed]
95. Kong, L.; Liu, J.; Zhou, Q.; Sun, Z.; Ma, Z. Sewage sludge derived biochars provoke negative effects on wheat growth related to the PTEs. *Biochem. Eng. J.* **2019**, *152*, 107386. [CrossRef]
96. Olszyk, D.M.; Shiroyama, T.; Novak, J.M.; Johnson, M.G. A rapid-test for screening biochar effects on seed germination. *Commun. Soil. Sci. Plant Anal.* **2018**, *49*, 2025–2041. [CrossRef]
97. Rogovska, N.; Laird, D.; Cruse, R.M.; Trabue, S.; Heaton, E. Germination Tests for Assessing Biochar Quality. *J. Environ. Qual.* **2012**, *41*, 1014–1022. [CrossRef]